ANL-HEP-PR-96-37

Isolated Prompt Photon Production in Hadronic Final States of e^+e^- Annihilation

Edmond L. Berger[1], Xiaofeng Guo[2], and Jianwei Qiu[2]

[1]*High Energy Physics Division, Argonne National Laboratory*

Argonne, Illinois 60439, USA

[2]*Department of Physics and Astronomy, Iowa State University*

Ames, Iowa 50011, USA

(May 15, 1996)

Abstract

We provide complete analytic expressions for the isolated prompt photon production cross section in e^+e^- annihilation reactions through one-loop order in quantum chromodynamics (QCD) perturbation theory. Functional dependences on the isolation cone size δ and isolation energy parameter ϵ are derived. The energy dependence as well as the full angular dependence of the cross section on θ_γ are displayed, where θ_γ specifies the direction of the photon with respect to the e^+e^- collision axis. We point out that conventional perturbative QCD factorization breaks down for isolated photon production in e^+e^- annihilation reactions in a specific region of phase space. We discuss the implications of this breakdown for the extraction of fragmentation functions from e^+e^- annihilation data and for computations of prompt photon production in hadron-hadron reactions.

12.38.Bx, 13.65.+i, 12.38.Qk

I. INTRODUCTION

The cross section for the inclusive yield of high energy photons in hadronic final states of e^+e^- annihilation is well-defined and, as demonstrated in our earlier paper [1], it may be calculated reliably within the context of quantum chromodynamics (QCD) perturbation theory. However, an important practical limitation of high energy investigations, whether in hadron-hadron reactions or e^+e^- annihilation processes, is that photons are observed and their cross sections are measured only when the photons are relatively isolated, separated to some extent in phase space from accompanying hadrons. Experimental procedures vary, but the essence of isolation is that a cone of half-angle δ is drawn about the direction of the photon's momentum, as sketched in Fig. 1, and the cross section is defined for photons accompanied by less than a specified amount of hadronic energy in the cone, *e.g.*, $E_h^{cone} \leq E_{\rm max} \equiv \epsilon_h E_\gamma$. In this paper, we undertake a thorough analysis of isolated prompt photon production in e^+e^- annihilation. Previous theoretical studies of isolated prompt photon production in $e^+e^- \to \gamma X$ include those of Refs. [2–5].

In this paper, our calculations of photon yields in $e^+e^- \to \gamma X$ are carried out through one-loop order. We compute explicitly direct photon production through first order in the electromagnetic coupling strength, α_{em}, and the quark-to-photon and gluon-to-photon fragmentation contributions through first order in the strong coupling strength α_s. We display the full angular dependence of the cross sections, separated into longitudinal $\sin^2\theta_\gamma$ and transverse components $(1+\cos^2\theta_\gamma)$, where θ_γ is the direction of the γ with respect to the e^+e^- collision axis.

A proper theoretical treatment of the isolated energetic photon yield requires careful consideration of the origins of both infrared and collinear singularities in QCD perturbation theory. In a theoretical calculation, photon isolation limits the final-state phase space accessible to accompanying gluons (g) and quarks (q). This phase space restriction breaks the perfect cancellation of soft singularities in each order of perturbation theory that guarantees reliable predictions in the inclusive case [5]. An uncanceled infrared singularity signals a

breakdown of conventional perturbative factorization. In this case, the uncanceled infrared singularity leads to an inverse-power divergence at the level of the partonic cross section [i.e., a $1/(1-x_1)$ divergence as $x_1 \to 1$] in the order α_s one-loop quark-to-photon fragmentation term. After convolution with the parton-to-photon fragmentation function, this inverse-power divergence becomes a logarithmic divergence in the isolated cross section.

Owing to isolation, the predicted photon cross section develops explicit functional dependence on the isolation parameters ϵ_h and δ. We show that at one-loop level, this cross section is well defined in most of phase space, so long as ϵ_h and δ are not too small. However, the region near $x_\gamma = 1/(1+\epsilon_h)$ is special, and the perturbatively calculated cross section is singular there; $x_\gamma = 2E_\gamma/\sqrt{s}$, where $\sqrt{s}$ denotes the center-of-mass energy of the e^+e^- reaction. In earlier papers [6], we presented analytic expressions for the dependence on isolation parameters in the specific case of photon production in hadron-hadron collisions [7–9]. In this paper, we provide a much more detailed treatment of photon isolation, concentrating on energetic photon production in electron-positron annihilation: $e^+e^- \to \gamma X$ [4,5].

In a perturbative QCD (pQCD) calculation of the inclusive yield of photons, the quark-photon collinear singularities that arise in each order of perturbation theory, associated with the hadronic component of the photon, are subtracted and absorbed into quark-to-photon and gluon-to-photon fragmentation functions, $D(z,\mu^2)$, in accord with the factorization theorem [10]. The scale μ^2 denotes the fragmentation scale that separates the non-perturbative domain from the region in which perturbation theory should apply; z is the momentum fraction carried by the observed photon from its parent parton. Since fragmentation is a process in which photons are part of quark, antiquark, or gluon "jets", it is evident that photon isolation reduces the contribution from fragmentation terms. For a small value of the energy resolution parameter, ϵ_h, the isolation cut eliminates most of the contribution from parton-to-photon fragmentation. However, ϵ_h may never be equal to zero either experimentally or theoretically. Experimentally, the finiteness of ϵ_h is guaranteed by detector resolution. Theoretically, the perturbative calculation of the cross section for isolated photons is ill defined if ϵ_h vanishes [6].

Fragmentation is modeled in perturbation theory as a collinear process, whereas experimental cone sizes are finite ($\delta \neq 0$) and partons are manifested as sprays of hadrons. Correspondingly, there is an inherent conceptual incompatibility between theoretical, collinear fragmentation functions and empirical fragmentation functions, $D_{\rm exp}\,(z, \mu^2, \delta)$, that more naturally would be defined with reference to a cone of specified size. In this paper, we limit ourselves to the usual collinear fragmentation functions, $D_{c\to\gamma}\,(z, \mu^2)$. We derive the expected dependence of the cross section on cone size δ and energy isolation ϵ_h, and we display a limited region of phase space in which the incompatibility of the collinear and finite cone size assumptions leads to collinear sensitivity of the isolated photon cross section. We discuss the impact of both infrared and collinear sensitivity on computations of prompt photon production in electron-positron and hadron-hadron reactions.

All four groups at LEP have published papers on prompt photon production [11]. A measurement of the photon fragmentation function from an analysis of the two-jet rate in Z decays is reported by the ALEPH collaboration [12]. Isolated prompt photon production has been treated theoretically previously, but our approach is different. In Ref. [2], the authors concentrate on events having a specific exclusive topology, such as a photon plus one hadronic jet; they discuss the extraction of the quark to photon fragmentation function from such data. In Ref. [3], isolated direct photon production through order α_{em} is treated; the fragmentation terms there are included only at lowest order, not through order α_s, and the angular dependence of the cross section is not derived. Practical aspects of confronting theoretical calculations with data from LEP are addressed in Ref. [13].

In Section II, we discuss the similarities and differences in the theoretical calculations of the cross sections for inclusive and isolated photons, and we provide a general factorized formula for the isolated photon cross section. Based on the definition of isolation, it is clear that the isolated photon cross section is part of the inclusive cross section. We write the isolated cross section as the inclusive cross section minus a subtraction term [6]. As in the calculation of jet cross sections [14], the singularity structure of subtraction term is much easier to deal with than that of the isolated cross section itself, at the order in perturba-

tion theory in which we are working. To establish notation, we derive explicit expressions for the isolated photon yield in lowest order ($O(\alpha_{em}^o)$, $O(\alpha_s^o)$). In Section III, we present our derivation of the three one-loop contributions to the subtraction terms. We work in $n = 4-2\epsilon$ dimensions in order to display singularities explicitly. The hard-scattering matrix elements are identical to those for the fully inclusive case discussed in Ref. [1], but the integration over momentum variables of the unobserved final-state partons is restricted by the requirements of photon isolation. All of our calculations are done analytically. In Section IV, we summarize our final expressions for the isolated photon cross section $E_\gamma d\sigma^{iso}_{e^+e^-\to\gamma X}/d^3\ell$, and we discuss the logarithmic divergence, $\ell n|(1+\epsilon_h) - 1/x_\gamma|$, associated with the limiting case in which x_γ approaches $1/(1+\epsilon_h)$. Numerical estimates, implications for isolated prompt photon phenomenology in e^+e^- and hadron-hadron reactions, thoughts for further work, and suggestions for comparisons with data are collected in Section V.

II. FACTORIZATION AND LOWEST ORDER CONTRIBUTION

In this section we drive a general factorized formula for the cross section for isolated photons, and we end the section with a computation of the lowest order $O(\alpha_{em}^o \alpha_s^o)$ contribution to the isolated energetic photon yield in $e^+e^- \to \gamma X$. The general notation in this paper is the same as that in Ref. [1].

A. Factorized Form for the Isolated Cross Section

With the assumption of parton-to-photon factorization, the cross section for an m parton final state in $e^+e^- \to \gamma X$, as sketched in Fig. 2, is

$$d\sigma^{(m)} = \frac{1}{2s}\left|\overline{M}_{e^+e^-\to \underbrace{c+\ldots}_{m}}\right|^2 dPS^{(m)} \cdot dz D_{c\to\gamma}(z). \tag{1}$$

Parton $c = \gamma, q, \bar{q}, g$, and $z = E_\gamma/E_c$. The factor $dPS^{(m)}$ is the m-parton phase space, and $D_{c\to\gamma}(z)$ is a function that describes fragmentation of parton c to the photon. This general expression is valid for both inclusive and isolated cross sections. The difference between the

inclusive and isolated cross sections resides in the phase space integration for the final state partons. For isolated cross sections, because of the isolation condition, not all partons can be integrated over all phase space. For example, partons with energy larger than $\epsilon_h E_\gamma$ are excluded from the cone of isolation about the observed photon.

As we proposed in Ref. [6], we write the isolated cross section as the following difference of cross sections:

$$E_\gamma \frac{d\sigma^{iso}_{e^+e^-\to\gamma X}}{d^3\ell} = E_\gamma \frac{d\sigma^{incl}_{e^+e^-\to\gamma X}}{d^3\ell} - E_\gamma \frac{d\sigma^{sub}_{e^+e^-\to\gamma X}}{d^3\ell}. \tag{2}$$

In Eq. (2), $E_\gamma d\sigma^{incl}/d^3\ell$ is the cross section for inclusive photons. It is well-defined in QCD perturbation theory and can be expressed in the following factorized form [1]

$$\begin{aligned} E_\gamma \frac{d\sigma^{incl}_{e^+e^-\to\gamma X}}{d^3\ell} &= \sum_c \int_{x_\gamma}^1 \frac{dz}{z^2}\, E_c \frac{d\hat{\sigma}^{incl}_{e^+e^-\to cX}}{d^3 p_c} \left(x_c = \frac{x_\gamma}{z}\right) D_{c\to\gamma}(z) \\ &\equiv \sum_c E_c \frac{d\hat{\sigma}^{incl}_{e^+e^-\to cX}}{d^3 p_c} \otimes D_{c\to\gamma}(z)\ , \end{aligned} \tag{3}$$

where $x_c = 2E_c/\sqrt{s}$, and the sum extends over $c = \gamma, q, \bar{q}$ and g. The short-distance hard-scattering cross sections $E_c d\hat{\sigma}^{incl}_{e^+e^-\to cX}/d^3 p_c$ in Eq. (3) are derived in Ref. [1] through one-loop level.

Cross sections for isolated photons $E_\gamma d\sigma^{iso}_{e^+e^-\to\gamma X}/d^3\ell$ measured, e.g., in LEP experiments, are well-behaved and finite. Therefore, the theoretical subtraction term $E_\gamma d\sigma^{sub}_{e^+e^-\to\gamma X}/d^3\ell$, defined in Eq. (2), should be well-behaved as well. Since the available phase space for the isolated photon cross section is smaller than that for inclusive photons, the cross section for isolated photons should be less than the corresponding inclusive cross section,

$$E_\gamma \frac{d\sigma^{iso}_{e^+e^-\to\gamma X}}{d^3\ell} \le E_\gamma \frac{d\sigma^{incl}_{e^+e^-\to\gamma X}}{d^3\ell}\ . \tag{4}$$

Consequently, the subtraction term, $E_\gamma d\sigma^{sub}_{e^+e^-\to\gamma X}/d^3\ell$, should be positive and finite. In terms of the definition given in Eq. (2), $E_\gamma d\sigma^{sub}_{e^+e^-\to\gamma X}/d^3\ell$ can be viewed as a "cross section" for a photon "jet" with photon momentum ℓ and hadronic energy in the "jet" cone E_h^{cone} restricted to be larger than $E_{\rm max} = \epsilon_h E_\gamma$. The virtue of Eq. (2) is that the infrared and

collinear singularities of the subtracted term σ^{sub} are much easier to deal with, at the order in which we are working, than those of σ^{iso} itself.

We assume as a working hypothesis that the subtraction term $\sigma^{sub}_{e^+e^-\to\gamma X}$ can be factored in the same way as the inclusive cross section and expressed as a convolution:

$$E_\gamma \frac{d\sigma^{sub}_{e^+e^-\to\gamma X}}{d^3\ell} = \sum_c \int_{x_\gamma}^1 \frac{dz}{z^2}\; E_c \frac{d\hat{\sigma}^{sub}_{e^+e^-\to cX}}{d^3 p_c}\left(x_c = \frac{x_\gamma}{z}\right) D^{iso}_{c\to\gamma}(z,\delta)\;. \tag{5}$$

In Eq. (5), we include explicit dependence on the cone size δ in the fragmentation functions in order to point out that, in principle, the fragmentation functions extracted from the cross section for isolated photons may depend on the definition of the isolation cone. Since the inclusive cross section σ^{incl} in Eq. (2) is well-defined in QCD perturbation theory, it is our principal task in this paper to show to what extent the short-distance subtraction terms $\hat{\sigma}^{sub}_{e^+e^-\to cX}$ are free from infrared and collinear divergences. As we show in Sec. IV, the conventional factorization Eq. (5) fails in the neighborhood of a well defined point in phase space, $x_\gamma = 2E_\gamma/\sqrt{s} = 1/(1+\epsilon_h)$.

The limits of integration over z in Eq. (5) are fixed by kinematics: $x_c = x_\gamma/z \le 1$. However, the isolation condition imposes, in addition, a requirement on the total hadronic energy in the isolation cone, $E_h^{cone} \ge E_{\rm max} = \epsilon_h E_\gamma$. Generally, E_h^{cone} has two sources: $E_{frag} + E_{partons}$, as is illustrated in Fig. 3. The fragmentation component, E_{frag}, is the hadronic component of the "jet" from which the energetic photon itself emerges. In the collinear approximation,

$$E_{frag} = (1-z)E_c = \left(\frac{1-z}{z}\right) E_\gamma. \tag{6}$$

The second component, $E_{partons}$, is contributed by other final state partons that are emitted into the region of phase space defined by the photon isolation cone. For the subtraction term,

$$\begin{aligned} E_h^{cone} &= E_{partons} + E_{frag} \\ &= E_{partons} + \left(\frac{1-z}{z}\right) E_\gamma \ge E_{\rm max} \equiv \epsilon_h E_\gamma. \end{aligned} \tag{7}$$

If $z \leq 1/(1+\epsilon_h)$, or, equivalently, $E_{frag} \geq \epsilon_h E_\gamma$, the constraint $E_h^{cone} \geq \epsilon_h E_\gamma$ is satisfied for any value of $E_{partons}$. Correspondingly, there is no restriction on the phase space for accompanying final state partons. Consequently, $\hat{\sigma}^{sub}_{e^+e^-\to cX} = \hat{\sigma}^{incl}_{e^+e^-\to cX}$ for $z \leq 1/(1+\epsilon_h)$.

If $z > 1/(1+\epsilon_h)$, to satisfy $E_h^{cone} \geq \epsilon_h E_\gamma$, it is necessary that

$$E_{partons} \geq E_{\max} - E_{frag} \equiv E_{\min}(z) = \left[(1+\epsilon_h) - \frac{1}{z}\right] E_\gamma. \tag{8}$$

We remark that $E_{\min}(z) > 0$ as long as $z > 1/(1+\epsilon_h)$, and $E_{\min}(z) = 0$ if $z = 1/(1+\epsilon_h)$.

Taking into account the constraints from the isolation condition, we can rewrite Eq. (5) as

$$\begin{aligned} E_\gamma \frac{d\sigma^{sub}_{e^+e^-\to\gamma X}}{d^3\ell} &= \sum_c \int_{\max\left[x_\gamma, \frac{1}{1+\epsilon_h}\right]}^1 \frac{dz}{z^2}\; E_c \frac{d\hat{\sigma}^{sub}_{e^+e^-\to cX}}{d^3 p_c}\left(x_c = \frac{x_\gamma}{z}\right)\Bigg|_{E_{partons}\geq E_{\min}} D^{iso}_{c\to\gamma}(z,\delta) \\ &+ \sum_c \int_{x_\gamma}^{\max\left[x_\gamma, \frac{1}{1+\epsilon_h}\right]} \frac{dz}{z^2}\; E_c \frac{d\hat{\sigma}^{incl}_{e^+e^-\to cX}}{d^3 p_c}\left(x_c = \frac{x_\gamma}{z}\right) D^{iso}_{c\to\gamma}(z,\delta) \\ &\equiv \sum_c \left[E_c \frac{d\hat{\sigma}^{sub}_{e^+e^-\to cX}}{d^3 p_c} \dot{\otimes} D^{iso}_{c\to\gamma}(z,\delta) + E_c \frac{d\hat{\sigma}^{incl}_{e^+e^-\to cX}}{d^3 p_c} \ddot{\otimes} D^{iso}_{c\to\gamma}(z,\delta)\right] . \end{aligned} \tag{9}$$

It is important to note in Eq. (9) that the short-distance subtraction terms $E_c d\hat{\sigma}^{sub}_{e^+e^-\to cX}/d^3p_c$ are needed only for $x_c \leq \min[x_\gamma(1+\epsilon_h), 1] < 1$, if $x_\gamma < 1/(1+\epsilon_h)$.

The modified convolution signs "$\dot{\otimes}$" and "$\ddot{\otimes}$" in Eq. (9) are defined in the same way as the convolution sign "$\otimes$" in Eq.(3), except for the limits of the z-integration. For functions $A(x_c)$ and $B(z)$, we define

$$A(x_c) \otimes B(z) \equiv \int_{x_\gamma}^1 \frac{dz}{z^2}\; A(x_c = x_\gamma/z)\; B(z)\;; \tag{10a}$$

$$A(x_c) \dot{\otimes} B(z) \equiv \int_{\max\left[x_\gamma, \frac{1}{1+\epsilon_h}\right]}^1 \frac{dz}{z^2}\; A(x_c = x_\gamma/z)\; B(z)\;; \tag{10b}$$

$$A(x_c) \ddot{\otimes} B(z) \equiv \int_{x_\gamma}^{\max\left[x_\gamma, \frac{1}{1+\epsilon_h}\right]} \frac{dz}{z^2}\; A(x_c = x_\gamma/z)\; B(z)\;. \tag{10c}$$

Notice the identity $\otimes = \dot{\otimes} + \ddot{\otimes}$.

Substituting Eqs. (3) and (9) into Eq. (2), we derive a simplified expression for the isolated cross section

$$E_\gamma \frac{d\sigma^{iso}_{e^+e^-\to\gamma X}}{d^3\ell} = \sum_c \int_{\max\left[x_\gamma, \frac{1}{1+\epsilon_h}\right]}^1 \frac{dz}{z^2} \left(E_c \frac{d\hat{\sigma}^{incl}_{e^+e^-\to cX}}{d^3p_c} - E_c \frac{d\hat{\sigma}^{sub}_{e^+e^-\to cX}}{d^3p_c}\bigg|_{E_{partons}\geq E_{\min}} \right) D_{c\to\gamma}(z)$$
$$= \sum_c \left(E_c \frac{d\hat{\sigma}^{incl}_{e^+e^-\to cX}}{d^3p_c} - E_c \frac{d\hat{\sigma}^{sub}_{e^+e^-\to cX}}{d^3p_c} \right) \dot{\otimes} D_{c\to\gamma}(z) \ . \tag{11}$$

In deriving Eq. (11), we assume for simplicity $D^{iso}_{c\to\gamma}(z,\delta) = D_{c\to\gamma}(z)$.

When $c=\gamma$, $D_{c\to\gamma}(z) = \delta(1-z)$ through order $O(\alpha_{em})$, and $E_{frag} = 0$ (i.e., $E_{\min} = \epsilon_h E_\gamma$). Therefore, we may rewrite Eq. (11) more explicitly as

$$E_\gamma \frac{d\sigma^{iso}_{e^+e^-\to\gamma X}}{d^3\ell} = E_\gamma \frac{d\hat{\sigma}^{iso}_{e^+e^-\to\gamma X}}{d^3\ell} + \sum_{c=q,\bar{q},g} E_c \frac{d\hat{\sigma}^{iso}_{e^+e^-\to cX}}{d^3p_c} \dot{\otimes} D_{c\to\gamma}(z) \ . \tag{12}$$

The isolated short-distance hard-scattering cross sections are defined as

$$E_\gamma \frac{d\hat{\sigma}^{iso}_{e^+e^-\to\gamma X}}{d^3\ell} \equiv E_\gamma \frac{d\hat{\sigma}^{incl}_{e^+e^-\to\gamma X}}{d^3\ell} - E_\gamma \frac{d\hat{\sigma}^{sub}_{e^+e^-\to\gamma X}}{d^3\ell}\bigg|_{\substack{partons\ inside\ cone;\\ E_{partons}\geq\epsilon_h E_\gamma.}} \tag{13a}$$

$$E_c \frac{d\hat{\sigma}^{iso}_{e^+e^-\to cX}}{d^3p_c} \equiv E_c \frac{d\hat{\sigma}^{incl}_{e^+e^-\to cX}}{d^3p_c} - E_c \frac{d\hat{\sigma}^{sub}_{e^+e^-\to cX}}{d^3p_c}\bigg|_{\substack{partons\ inside\ cone;\\ E_{partons}\geq E_{\min}.}}. \tag{13b}$$

The value of $E_{\min}$ is specified in Eq. (8).

Anticipating a result to be derived below, we remark that when $x_\gamma \to 1/(1+\epsilon_h)$, the subtraction term $\hat{\sigma}^{sub}$ and, consequently, the isolated cross section $\hat{\sigma}^{iso}$ develop a logarithmic singularity, $\ell n|(1+\epsilon_h) - 1/x_\gamma|$. We discuss this singularity in detail in Section IV D.

B. Derivation of the Lowest Order Contribution

In lowest order, $O\left(\alpha^o_{em}\alpha^o_s\right)$, photon production occurs only through the quark or anti-quark fragmentation process sketched in Fig. 4. In this case $c = q, \bar{q}$, and $x_c = 2E_c/\sqrt{s} = 1$ in Eq. (11); and there is no direct production of photons. Owing to momentum balance, the quark and anti-quark have equal but opposite momentum in the overall center-of-mass system, and there can be no accompanying parton in the isolation cone around the fragmenting parton, i.e., $E_{partons} = 0$ inside the cone. Therefore, at $O\left(\alpha^0_{em}\alpha^0_s\right)$,

$$E_c \frac{d\hat{\sigma}^{(0)sub}_{e^+e^-\to cX}}{d^3p_c}\bigg|_{\substack{partons\ inside\ cone;\\ E_{partons}\geq E_{\min}.}} = 0 \ . \tag{14}$$

Substituting Eq. (14) into Eq. (11), we derive

$$E_\gamma \frac{d\sigma^{(0)iso}_{e^+e^-\to\gamma X}}{d^3\ell} = \int_{\max\left[x_\gamma, \frac{1}{1+\epsilon_h}\right]}^1 \frac{dz}{z^2} \sum_{c=q,\bar{q}} E_c \frac{d\hat{\sigma}^{(0)incl}_{e^+e^-\to cX}}{d^3p_c}\left(x_c = \frac{x_\gamma}{z}\right) D_{c\to\gamma}(z). \tag{15}$$

The lowest order hard-scattering cross section $E_c d\hat{\sigma}^{(0)incl}_{e^+e^-\to cX}/d^3p_c$ in n dimensions is derived in our earlier paper [1]:

$$E_c \frac{d\hat{\sigma}^{(0)incl}_{e^+e^-\to cX}}{d^3p_c} = \left[\frac{2}{s}F_c^{PC}(s)\right] \alpha_{em}^2 N_c \left(\frac{4\pi\mu^2}{(s/4)\sin^2\theta_c}\right)^\epsilon \frac{1}{\Gamma(1-\epsilon)}\left[\left(1+\cos^2\theta_c\right) - 2\epsilon\right] \frac{\delta(x_c-1)}{x_c}, \tag{16}$$

with $\epsilon = (4-n)/2$, and $c = q, \bar{q}$. The angle θ_c is the scattering angle of parton c with respect to the e^+e^- collision axis in the overall center-of-mass frame. The normalization factor is $(2/s)F_q^{PC}(s)$ is [1]

$$\frac{2}{s}F_q^{PC}(s) = \frac{1}{s^2}\left[\, e_q^2 + \left(|v_e|^2 + |a_e|^2\right)\left(|v_q|^2 + |a_q|^2\right) \frac{s^2}{\left(s-M_Z^2\right)^2 + M_Z^2\Gamma_Z^2} - 2e_q v_e v_q \frac{s\left(s-M_Z^2\right)}{\left(s-M_Z^2\right)^2 + M_Z^2\Gamma_Z^2}\right]. \tag{17}$$

In Eq. (17), both γ and Z° intermediate state contributions are represented, including their interference. The vector (v) and axial-vector (a) couplings are defined through $ie\gamma^\mu(v_f + a_f\gamma_5)$, the vertex coupling between the intermediate vector boson and the initial/final fermion pair of flavor f [1].

At this order, the cross section is manifestly finite in the limit $\epsilon \to 0$, and we may set $\epsilon = 0$ directly in Eq. (16). Nevertheless, Eq. (16) expressed in n dimensions is valuable for later comparison with the higher order cross section. Substituting Eq. (16) into Eq. (15), we obtain the lowest order isolated cross section [4]

$$E_\gamma \frac{d\sigma^{(0)iso}_{e^+e^-\to\gamma X}}{d^3\ell} = 2\sum_q \left[\frac{2}{s}F_q^{PC}(s)\right] \alpha_{em}^2 N_c (1+\cos^2\theta_\gamma) \frac{1}{x_\gamma} D_{q\to\gamma}(x_\gamma, \mu_F), \tag{18}$$

for $x_\gamma \geq 1/(1+\epsilon_h)$. At this order, the isolated cross section vanishes if $x_\gamma < 1/(1+\epsilon_h)$. The angles θ_γ and θ_c are identical since we take all products of the fragmentation to be collinear. The overall factor of 2 in Eq. (18) accounts for the $\bar{q}$ contribution. Our result in Eq. (18) is consistent with those derived in Refs. [2,3].

III. SUBTRACTION TERMS AT ONE-LOOP ORDER

Having calculated the cross section for inclusive photon production in Ref. [1], we must calculate the subtraction terms defined in Eqs. (2) and (13) in order to derive the complete expression for the isolated photon cross section. As in the inclusive case, there are three distinct contributions to the subtraction terms for $e^+e^- \to \gamma X$ at one-loop level in perturbation theory:

$$e^+e^- \to \gamma, \qquad O(\alpha_{em}) \tag{19a}$$

$$e^+e^- \to q \text{ (or } \bar{q}) \to \gamma, \qquad O(\alpha_s) \tag{19b}$$

and

$$e^+e^- \to g \to \gamma. \qquad O(\alpha_s) \tag{19c}$$

In Eqs. (19b) and (19c), we have in mind contributions from quark (or antiquark) and gluon fragmentation to photons in the three-parton final state process $e^+e^- \to q\bar{q}g$. The first contribution, Eq. (19a), arises from $e^+e^- \to q\bar{q}\gamma$ where the γ is <u>not</u> collinear with either $\bar{q}$ or q.

In this section we derive and present explicit expressions for the contributions to $E_\gamma d\sigma^{sub}_{e^+e^-\to\gamma X}/d^3\ell$ from each of the three processes in Eq. (19).

A. Factorized Form for the Short-Distance Hard Parts: $\hat{\sigma}^{sub}$

To calculate the short-distance partonic cross sections (hard parts), $\hat{\sigma}^{sub}$ in Eq. (13), we first apply the factorized form in Eq. (9) to parton states perturbatively order-by-order in the coupling constants, and we then extract the perturbative expressions for $\hat{\sigma}^{sub}$. We illustrate this procedure in this subsection for each of the processes in Eq. (19)

The Feynman graphs for $\sigma^{(1)sub}_{e^+e^-\to\gamma X}$ are sketched in Fig. 5. To derive the direct production term corresponding to Eq. (19a), $\hat{\sigma}^{(1)sub}_{e^+e^-\to\gamma X}$, we apply Eq. (9) perturbatively to first order in α_{em}. We obtain

$$\sigma^{(1)sub}_{e^+e^-\to\gamma X}\Big|_{E_q(or E_{\bar q})\geq\epsilon_h E_\gamma} = \hat\sigma^{(1)sub}_{e^+e^-\to\gamma X}(x_\gamma)\dot\otimes D^{(0)}_{\gamma\to\gamma}(z) + \hat\sigma^{(1)incl}_{e^+e^-\to\gamma X}(x_\gamma)\ddot\otimes D^{(0)}_{\gamma\to\gamma}(z)$$
$$+ \hat\sigma^{(0)sub}_{e^+e^-\to qX}(x_q)\dot\otimes D^{(1)}_{q\to\gamma}(z) + \hat\sigma^{(0)incl}_{e^+e^-\to qX}(x_q)\ddot\otimes D^{(1)}_{q\to\gamma}(z)$$
$$+ (q\to\bar q)\ . \tag{20}$$

The zeroth order subtraction term $\hat\sigma^{(0)sub}_{e^+e^-\to cX}$ vanishes, as shown in Eq. (14). Since the zeroth order photon-photon fragmentation function $D^{(0)}_{\gamma\to\gamma}(z) = \delta(1-z)$, and $\hat\sigma^{(1)incl}_{e^+e^-\to\gamma X}(x_\gamma)\ddot\otimes D^{(0)}_{\gamma\to\gamma}(z)$ vanishes, the expression for the short-distance hard part becomes

$$\hat\sigma^{(1)sub}_{e^+e^-\to\gamma X}(x_\gamma) = \sigma^{(1)sub}_{e^+e^-\to\gamma X}\Big|_{E_q(or E_{\bar q})\geq\epsilon_h E_\gamma} - \hat\sigma^{(0)incl}_{e^+e^-\to qX}(x_q)\ddot\otimes D^{(1)}_{q\to\gamma}(z) - (q\to\bar q)\ , \tag{21}$$

where the terms with the minus sign are often called collinear counter-terms. In this equation, $\hat\sigma^{(0)incl}_{e^+e^-\to qX}$ is obtained from Eq. (16), and the modified convolution "$\ddot\otimes$" is defined in Eq. (10c). The perturbative fragmentation function $D^{(1)}_{q\to\gamma}(z)$ in n-dimensions can be calculated by evaluating the diagram in Fig. 6. We obtain [1]

$$D^{(1)}_{q\to\gamma}(z) = e_q^2\ \left(\frac{\alpha_{em}}{2\pi}\right)\frac{1+(1-z)^2}{z}\ \left(\frac{1}{-\epsilon}\right); \tag{22}$$

and $D^{(1)}_{\bar q\to\gamma}(z) = D^{(1)}_{q\to\gamma}(z)$. Although $\sigma^{(1)sub}_{e^+e^-\to\gamma X}$ and the perturbative fragmentation functions $D^{(1)}_{q(\mathrm{or}\,\bar q)\to\gamma}(z)$ are both formally divergent as $\epsilon\to 0$, these divergences cancel and leave a finite expression for $\hat\sigma^{(1)sub}_{e^+e^-\to\gamma X}$, if the conventional QCD factorization theorem holds [10].

For the gluon fragmentation contribution: $e^+e^-\to g\to\gamma$ (Eq. (19c)), we apply Eq. (9) to a gluon state perturbatively to first order in α_s. Letting E_g be the gluon's energy, we obtain

$$\sigma^{(1)sub}_{e^+e^-\to gX}\Big|_{E_q(or E_{\bar q})\geq\epsilon_{\min}E_g} = \hat\sigma^{(1)sub}_{e^+e^-\to gX}(x_g)\dot\otimes D^{(0)}_{g\to g}(z) + \hat\sigma^{(1)incl}_{e^+e^-\to gX}(x_g)\ddot\otimes D^{(0)}_{g\to g}(z)$$
$$+ \hat\sigma^{(0)sub}_{e^+e^-\to qX}(x_q)\dot\otimes D^{(1)}_{q\to g}(z) + \hat\sigma^{(0)incl}_{e^+e^-\to qX}(x_q)\ddot\otimes D^{(1)}_{q\to g}(z)$$
$$+ (q\to\bar q)\ , \tag{23}$$

where $x_g = 2E_g/\sqrt{s}$, and $x_q = 2E_q/\sqrt{s}$. In Eq. (23), the modified convolutions are defined in the same way as in Eq. (10), except that x_γ is replaced by x_g, and ϵ_h is replaced by $\epsilon_{\min}$;

$$\epsilon_{\min}(z) \equiv \frac{E_{\min}(z)}{E_g}$$
$$= (1+\epsilon_h)z - 1 \geq 0\ , \tag{24}$$

where $z = x_\gamma/x_g$. Because $z \leq 1$, we note the restrictions

$$\epsilon_{\rm min}(z) \leq \epsilon_h \ ; \quad \text{or} \quad \frac{1}{1+\epsilon_{\rm min}} \geq \frac{1}{1+\epsilon_h} \ . \tag{25}$$

Since $D^{(0)}_{g\to g}(z) = \delta(1-z)$, and $\hat{\sigma}^{(0)sub}_{e^+e^-\to qX}(x_q) = 0$, Eq. (23) can be rewritten as

$$\hat{\sigma}^{(1)sub}_{e^+e^-\to gX}(x_g) = \sigma^{(1)sub}_{e^+e^-\to gX}\Big|_{E_q(or E_{\bar{q}})\geq \epsilon_{\rm min}E_g} - \hat{\sigma}^{(0)incl}_{e^+e^-\to qX}(x_q)\ddot{\otimes} D^{(1)}_{q\to g} - (q\to\bar{q}). \tag{26}$$

In Eq. (26), the divergent cross section $\sigma^{(1)sub}_{e^+e^-\to gX}$ is evaluated from the Feynman graphs shown in Fig. 7, and the quark-to-gluon collinear divergences are embedded in the first-order fragmentation function $D^{(1)}_{q\to g}$. The function $D^{(1)}_{q\to g}$ is the same as $D^{(1)}_{q\to\gamma}$ of Eq. (22), except that $e_q^2(\alpha_{em}/2\pi)$ is replaced by $C_F(\alpha_s/2\pi)$. The color factor $C_F = 4/3$.

For the quark fragmentation contribution: $e^+e^- \to q \to \gamma$ (Eq. (19b)), we apply Eq. (9) to a quark state perturbatively at first order in α_s. In a fashion similar to the derivation of $\hat{\sigma}^{(1)sub}_{e^+e^-\to gX}$, we derive the short-distance hard part for quark fragmentation

$$\hat{\sigma}^{(1)sub}_{e^+e^-\to qX}(x_q) = \sigma^{(1)sub}_{e^+e^-\to qX}\Big|_{E_g(or E_{\bar{q}})\geq \epsilon_{\rm min}E_q} - \hat{\sigma}^{(0)incl}_{e^+e^-\to q'}(x_{q'})\ddot{\otimes} D^{(1)}_{q'\to q}(z) \ . \tag{27}$$

The Feynman graphs that contribute to $\sigma^{(1)sub}_{e^+e^-\to qX}$ are sketched in Fig. 8. In this fragmentation process, the quark is effectively "observed" through $q \to \gamma$ fragmentation. For the real gluon emission diagrams, sketched in Fig. 8a, the gluon and antiquark are not observed and their momenta will be integrated over. Since $\epsilon_{\rm min}(z)$, defined in Eq. (24), can be equal to zero, the contribution of the real emission diagrams to $\sigma^{(1)sub}_{e^+e^-\to qX}$ shows both infrared and collinear singularities. The infrared singularity associated with soft gluon emission should be canceled by a contribution from the virtual gluon exchange diagrams shown in Fig. 8b, if the conventional QCD factorization theorem holds. When the gluon is parallel to the fragmenting quark, the real emission diagrams manifest a collinear singularity that should be canceled by the negative term in Eq. (27).

The perturbative fragmentation function $D^{(1)}_{q\to q}(z)$ in Eq. (27) is determined from Feynman diagrams sketched in Fig. 9. In n-dimensions, we obtain [1]

$$D^{(1)}_{q\to q}(z) = C_F\left(\frac{\alpha_s}{2\pi}\right)\left[\frac{1+z^2}{(1-z)_+} + \frac{3}{2}\delta(1-z)\right]\left(\frac{1}{-\epsilon}\right) \ , \tag{28}$$

where the "+" description is defined as usual,

$$\left(\frac{1}{1-z}\right)_+ \equiv \frac{1}{1-z} - \delta(1-z)\int_0^1 dz'\ \frac{1}{1-z'}. \tag{29}$$

B. Parton Level Cross Sections: $\sigma^{(1)sub}$

In order to derive the short-distance hard parts at one-loop level, defined in Eqs. (21), (26) and (27), we must compute the formally divergent partonic cross sections $\sigma^{(1)sub}_{e^+e^-\to cX}$ in n-dimensions, for $c = \gamma$, g, q and $\bar{q}$. We must evaluate Feynman diagrams for e^+e^- to three particle final states, $(q\bar{q}\gamma)$ or $(q\bar{q}g)$; and e^+e^- to two particle final states $(q\bar{q})$ with one-loop virtual gluon exchange. As derived in Ref. [1], the general expression for the partonic cross section is

$$d\sigma^{(1)sub} = \sum_{q,m}\left[\frac{2}{s}F_q^{PC}(s)\right]\ e^2\ C_q\ \frac{1}{4}(H_1+H_2)\ dPS^{(m)sub}, \tag{30}$$

where $m = 2$ or 3 corresponding to the number of final state particles, and the constant C_q is an overall color factor. In Eq. (30), the functions H_1 and H_2 are defined by

$$H_1 = -g_{\mu\nu}\ H^{\mu\nu}, \qquad H_2 = -\frac{k_\mu k_\nu}{q^2}\ H^{\mu\nu}. \tag{31}$$

Function $H^{\mu\nu}$ is the hadronic tensor, and q^μ (k^μ) is the sum (difference) of the incoming e^+ and e^- momenta. The factor $dPS^{(m)sub}$ in Eq. (30) is the multi-particle phase space element. In $n = 4-2\epsilon$ dimensions we obtain [1]

$$dPS^{(2)sub} = \frac{1}{2}\frac{1}{(2\pi)^3}\frac{d^3p_i}{E_i}\left(\frac{4\pi}{(s/4)\sin^2\theta_i}\right)^\epsilon \frac{1}{\Gamma(1-\epsilon)}\frac{2\pi}{s}\frac{\delta\left(x_i-1\right)}{x_i} \tag{32}$$

for the two-body final state with parton i being observed; and

$$\begin{aligned} dPS^{(3)sub} = {} & \frac{1}{2}\frac{1}{(2\pi)^3}\frac{d^3p_i}{E_i}\left(\frac{4\pi}{(s/4)\sin^2\theta_i}\right)^\epsilon \frac{1}{\Gamma(1-\epsilon)}\frac{2\pi}{s}\frac{\delta\left(x_i-(1-y_{jh})\right)}{x_i} \\ & \times \frac{s}{4}\left[\left(\frac{1}{2\pi}\right)^2\left(\frac{4\pi}{s}\right)^\epsilon \frac{1}{\Gamma(1-\epsilon)}\frac{d\Omega_{n-3}(p_j)}{\Omega_{n-3}}\right] \\ & \times \frac{dy_{12}}{y_{12}^\epsilon}\,\frac{dy_{13}}{y_{13}^\epsilon}\,\frac{dy_{23}}{y_{23}^\epsilon}\,\delta\left(1-y_{12}-y_{13}-y_{23}\right), \end{aligned} \tag{33}$$

for the three-body final states. In Eq. (33), we use labels "1", "2", and "3" for the final-state q, $\bar{q}$ and γ (or g), respectively; and we use label "i" (=1,2 or 3) to designate the "observed" one. Symbol "j"($\neq i$) labels the particle over whose momentum we integrate, and the momentum of "h"($\neq i \neq j$) is fixed by the momentum conservation δ-function. In Eq. (33), $\Omega_{n-3} = 2\pi^{(1-\epsilon)}/\Gamma(1-\epsilon)$. The dimensionless invariants x_i and y_{ij} in Eq. (33) are defined as

$$x_i \equiv \frac{2E_i}{\sqrt{s}}\,, \qquad y_{ij} \equiv \frac{2p_i \cdot p_j}{s}, \tag{34}$$

with $i, j = 1, 2, 3$.

The multi-particle phase space expressions in Eqs. (32) and (33), are formally identical to those for our calculation of the inclusive cross section [1], except that the limits of integration differ here, owing to the isolation condition. These phase space limits are derived below for each individual subprocess.

As indicated in Figs. 5, 7 and 8, all three one-loop partonic cross sections have the same e^+e^- to three-body matrix elements. However, the quark fragmentation cross section has an extra contribution from virtual gluon exchange diagrams. We derive the functions H_1 and H_2 appearing in Eq. (30) by evaluating the square of the matrix element for the Feynman diagrams in Fig. 5 (or Fig. 7, or Fig. 8a).

$$\begin{aligned} H_1 &= 8(1-\epsilon)\left\{(1-\epsilon)\left[\frac{y_{13}}{y_{23}}+\frac{y_{23}}{y_{13}}\right]+2\left[\frac{y_{12}}{y_{13}y_{23}}-\epsilon\right]\right\}; \\ H_2 &= -4\left\{(1-\epsilon)\left[\frac{y_{13}}{y_{23}}+\frac{y_{23}}{y_{13}}\right]+2\left[\frac{y_{12}}{y_{13}y_{23}}-\epsilon\right]\right\} \\ &\quad +\frac{4}{y_{13}y_{23}}\left[y_{1k}^2+y_{2k}^2\right]-\frac{4\epsilon}{y_{13}y_{23}}\,y_{3k}^2. \end{aligned} \tag{35}$$

We temporarily omit overall coupling factors of $e_q^2\,(e\mu^\epsilon)^4$ for $(q\bar{q}\gamma)$ and $(e\mu^\epsilon)^2(g\mu^\epsilon)^2$ for $(q\bar{q}g)$. The invariants y_{ik} with $i = 1, 2, 3$ are defined as

$$y_{ik} \equiv \frac{2p_i \cdot k}{s}. \tag{36}$$

The identity

$$y_{1k} + y_{2k} + y_{3k} = 0 \tag{37}$$

follows from the equalities $k \cdot q = 0$ and $q = p_1 + p_2 + p_3$.

We choose to work in the overall center of mass frame, sketched in Fig. 10, when integrating H_1 and H_2 over three-body phase space. Letting θ_{ik} be the polar angle of the observed parton momentum p_i with respect to the momentum k, and angle θ_{jx} the n-dimensional generalization of the three-dimensional azimuthal angle ϕ, defined through p_j, we derive general expressions for the three y_{ik} [1].

$$\begin{aligned}
y_{ik} &= -x_i \cos\theta_{ik}; \\
y_{jk} &= -\left[\frac{y_{ih}y_{jh} - y_{ij}}{x_i}\right]\cos\theta_{ik} - \left[\frac{2\sqrt{y_{ij}y_{ih}y_{jh}}}{x_i}\right]\sin\theta_{ik}\cos\theta_{jx}; \\
y_{hk} &= -\left[\frac{y_{ij}y_{jh} - y_{ih}}{x_i}\right]\cos\theta_{ik} + \left[\frac{2\sqrt{y_{ij}y_{ih}y_{jh}}}{x_i}\right]\sin\theta_{ik}\cos\theta_{jx}.
\end{aligned} \tag{38}$$

These general expressions satisfy the identity in Eq. (37). In the reference frame we are using,

$$d\Omega_{n-3}(p_j) = d\cos\theta_{jx}\ (1-\cos^2\theta_{jx})^{\frac{n-5}{2}}\ d\Omega_{n-4}(p_j)\ . \tag{39}$$

Since we choose the photon direction to define the z-axis (Fig. 10), with our cone definition, the range of the azimuthal angle θ_{jx} integration should not be affected by the isolation cut. Therefore, just as the inclusive case [1], the integral over $d\cos\theta_{jx}$ is done from $\cos\theta_{jx} = -1$ to $+1$ when H_2 is integrated over phase space. The expression for three-body phase space, Eqs. (33) and (39), is an even function of $\cos\theta_{jx}$. Correspondingly, terms in H_2 that are odd functions of $\cos\theta_{jx}$ do not survive after integration. Because H_2 (Eq. (35)) depends only on the square of y_{1k} and y_{2k}, after eliminating all terms linear in $\cos\theta_{jx}$, we find that the only remaining dependence on θ_{jx} in H_2 is of the form $\cos^2\theta_{jx}$. We may integrate over θ_{jx} independently of other variables, or, equivalently, we may replace $\cos^2\theta_{jx}$ in H_2 by its average in n-dimensions and thereby eliminate θ_{jx} dependence in H_2 completely.

The average of $\cos^2\theta_{jx}$ in n-dimensions is [1]

$$< \cos^2\theta_{jx} >_{n-dim} = \frac{1}{2(1-\epsilon)}. \tag{40}$$

We use Eq. (40) to replace $\cos^2\theta_{jx}$ in H_2 by $1/2(1-\epsilon)$, and we denote the resulting expression H_2^{eff}.

In following subsections, for a given observed particle (e.g. γ or q), we derive expressions for y_{ik}^2, for $i = 1, 2, 3$, substitute these y_{ik}^2 into Eq. (35), replace $\cos^2\theta_{jx}$ by $1/2(1-\epsilon)$ to obtain $(H_1 + H_2^{eff})$, and finally, substitute these $(H_1 + H_2^{eff})$ into Eq. (30) to get the partonic cross sections: $\sigma^{(1)sub}$.

C. Derivation of $\hat{\sigma}^{(1)sub}_{e^+e^-\to\gamma X}$

In this subsection we present an explicit derivation of the finite hard-scattering cross section $\hat{\sigma}^{(1)sub}_{e^+e^-\to\gamma X}$ at order α_{em}, as expressed in Eq. (21).

Since the photon is the observed particle, we set $i = 3$. The assignment of j and h is arbitrary and has no effect on the final result owing to symmetry between the quark and antiquark. We choose $j = 1$ and $h = 2$; i.e., "1" for the quark, and "2" for the antiquark. Referring to Eq. (34), we remark that y_{13} is proportional to the invariant mass of the photon and quark system. Starting from Eq. (38), and after using Eq. (40), we obtain the effective expressions

$$\begin{aligned}
y_{3k}^2 &= \; x_3^2\cos^2\theta_3;\\
y_{1k}^2 &= \left[\frac{y_{23}y_{12}-y_{13}}{x_3}\right]^2\cos^2\theta_3 + \frac{1}{1-\epsilon}\left[\frac{2(y_{12}y_{13}y_{23})}{x_3^2}\right]\sin^2\theta_3;\\
y_{2k}^2 &= \left[\frac{y_{13}y_{12}-y_{23}}{x_3}\right]^2\cos^2\theta_3 + \frac{1}{1-\epsilon}\left[\frac{2(y_{12}y_{13}y_{23})}{x_3^2}\right]\sin^2\theta_3.
\end{aligned} \tag{41}$$

Substituting these y_{ik}^2, with $i = 1, 2, 3$, into Eq. (35), we derive

$$\begin{aligned}
\frac{1}{4}\left(H_1 + H_2^{eff}\right) = e_q^2(e\mu^\epsilon)^4 \Bigg\{ & \left(1+\cos^2\theta_3 - 2\epsilon\right)\left[(1-\epsilon)\left(\frac{y_{13}}{y_{23}}+\frac{y_{23}}{y_{13}}\right) + 2\left(\frac{y_{12}}{y_{13}y_{23}} - \epsilon\right)\right]\\
& + \left(1-3\cos^2\theta_3\right)\left[\frac{4y_{12}}{x_3^2}\right]\Bigg\}\\
= e_q^2(e\mu^\epsilon)^4 \Bigg\{ & \left(1+\cos^2\theta_3 - 2\epsilon\right)\left[\frac{1+(1-x_3)^2}{x_3^2}\right]\left(\frac{1}{\hat{y}_{13}}+\frac{1}{\hat{y}_{23}}\right)\\
& + \left(1+\cos^2\theta_3 - 2\epsilon\right)\left[-2 - \epsilon\left(\frac{1}{\hat{y}_{13}}+\frac{1}{\hat{y}_{23}}\right)\right]
\end{aligned}$$

$$+\left(1-3\cos^2\theta_3\right)\left[\frac{4(1-x_3)}{x_3^2}\right]\Bigg\}. \tag{42}$$

In Eq. (42), we introduce the overall coupling factor and neglect terms that do not contribute in the limit $\epsilon \to 0$. The variable $\hat{y}_{j3}$ with $j = 1, 2$ is defined as $\hat{y}_{j3} = y_{j3}/x_3$; x_3 is the same as x_γ, and θ_3 is equal to θ_γ in this case.

The two δ functions in $dPS^{(3)}$, Eq. (33), are used to do the dy_{12} and dy_{23} integrations, and y_{13} is left as the integration variable. Different choices of the integration variable are of course equivalent. In terms of y_{13} and x_3, we have identities

$$y_{12} = 1 - x_3, \qquad y_{23} = x_3 - y_{13}. \tag{43}$$

The limits of integration over y_{13} are derived from the isolation requirement for the subtraction terms. In our parton level approach, hadronic energy in the isolation cone means a parton must be present inside the isolation cone of observed photon. Second, this hadronic energy must be larger than $\epsilon_h E_\gamma$. We use δ to denote the half angle of the isolation cone. The statement that the quark (parton "1") is inside the isolation cone provides the relationship

$$\hat{y}_{23} \geq \frac{\cos^2(\delta/2)}{1 - x_3\sin^2(\delta/2)}, \tag{44}$$

whereas the statement that the antiquark (parton "2") is inside the isolation cone leads to

$$\hat{y}_{13} \geq \frac{\cos^2(\delta/2)}{1 - x_3\sin^2(\delta/2)}. \tag{45}$$

Using Eq. (43) and $0 \leq y_{13} \leq x_3$, we derive the condition that either the quark or the antiquark is inside the isolation cone:

$$\begin{aligned} 0 \quad \leq \quad \hat{y}_{13} \quad \leq \quad & \frac{(1-x_3)\sin^2(\delta/2)}{1 - x_3\sin^2(\delta/2)} \ ; \\ \frac{\cos^2(\delta/2)}{1 - x_3\sin^2(\delta/2)} \quad \leq \quad & \hat{y}_{13} \quad \leq \quad 1. \end{aligned} \tag{46}$$

These two regions of the $\hat{y}_{13}$ integration do not overlap as long as $x_3 > 1 - \cot^2(\delta/2)$.

The second part of the isolation constraint is the requirement that the parton's energy inside the isolation cone be larger than $\epsilon_h E_\gamma$. We derive

$$\begin{aligned}
\max[0,(1+\epsilon_h-1/x_3)] \quad &\leq \quad \hat{y}_{13} \quad \leq \quad \frac{(1-x_3)\sin^2(\delta/2)}{1-x_3\sin^2(\delta/2)}\ , \\
1-\frac{(1-x_3)\sin^2(\delta/2)}{1-x_3\sin^2(\delta/2)} \quad &\leq \quad \hat{y}_{13} \quad \leq \quad \min[1,1-(1+\epsilon_h-1/x_3)]\ . \qquad (47)
\end{aligned}$$

For simplicity of notation and to facilitate comparison of our results with those of Ref. [3], we define

$$\begin{aligned}
y_c &\equiv \frac{(1-x_3)\sin^2(\delta/2)}{1-x_3\sin^2(\delta/2)} \quad \Rightarrow \quad (1-x_3)\frac{\delta^2}{4}, \\
y_m &\equiv 1+\epsilon_h-\frac{1}{x_3}. \qquad (48)
\end{aligned}$$

Henceforth in this subsection, we set $x_3 = x_\gamma$. The first of the conditions in Eq. (47) indicates that y_m should be less than y_c. Therefore, the subtraction term should vanish if $y_m \geq y_c$, i.e.,

$$E_\gamma \frac{\hat{\sigma}^{(1)sub}_{e^+e^-\to\gamma X}}{d^3\ell} = 0 \quad \text{if} \quad x_\gamma \geq x_\gamma^{\max}(\delta,\epsilon_h)\ . \qquad (49)$$

Here, $x_\gamma^{\max}(\delta,\epsilon_h)$ is expressed as

$$x_\gamma^{\max}(\delta,\epsilon_h) \equiv \left(\frac{1}{1+\epsilon_h}\right)\frac{2}{1+\sqrt{1-4\epsilon_h\sin^2(\delta/2)/(1+\epsilon_h)^2}}. \qquad (50)$$

We note that

$$x_\gamma^{\max}(\delta,\epsilon_h) \geq \frac{1}{1+\epsilon_h} \qquad (51)$$

if $\delta \neq 0$. We define

$$\Delta \equiv x_\gamma^{\max}(\delta,\epsilon_h) - \frac{1}{1+\epsilon_h} \simeq \epsilon_h\,\frac{\delta^2}{4}\ , \qquad (52)$$

where we expand $x_\gamma^{\max}(\delta,\epsilon_h)$ of Eq. (51) for small δ. For $\delta = 20^\circ$, typical of LEP experiments, $\Delta \simeq 0.03\epsilon_h$. The interval between the critical value $x_\gamma = 1/(1+\epsilon_h)$ and $x_\gamma^{\max}$ is consequently very small. Equation (49) is actually a condition due to energy-momentum conservation.

We consider next, in turn, the regions $x_\gamma \leq 1/(1+\epsilon_h)$ and $x_\gamma > 1/(1+\epsilon_h)$. If $x_\gamma \leq 1/(1+\epsilon_h)$, the integration over $\hat{y}_{13}$ for $d\sigma^{(1)sub}$ has two separate intervals, defined in Eq. (47),

$$\int d\hat{y}_{13} \Rightarrow \int_0^{y_c} d\hat{y}_{13} + \int_{1-y_c}^1 d\hat{y}_{13}. \tag{53}$$

Substituting Eq. (42) into Eq. (30), and performing this $\hat{y}_{13}$ integration, we derive parton level cross section

$$\begin{aligned} E_\gamma \frac{d\sigma^{(1)sub}_{e^+e^-\to\gamma X}}{d^3\ell} = & \; 2\sum_q \left[\frac{2}{s} F_q^{PC}(s)\right] \left[\alpha_{em}^2 N_c \left(\frac{4\pi\mu^2}{(s/4)\sin^2\theta_\gamma}\right)^\epsilon \frac{1}{\Gamma(1-\epsilon)}\right] \frac{1}{x_\gamma} e_q^2 \left(\frac{\alpha_{em}}{2\pi}\right) \\ & \times \left\{ (1+\cos^2\theta_\gamma - 2\epsilon) \left(\frac{1+(1-x_\gamma)^2}{x_\gamma}\right) \left(-\frac{1}{\epsilon}\right) \right. \\ & + (1+\cos^2\theta_\gamma) \left[\left(\frac{1+(1-x_\gamma)^2}{x_\gamma}\right) \left(\ell n\left(\frac{s}{\mu^2_{\overline{\rm MS}}}\right) + \ell n(x_\gamma^2(1-x_\gamma)) + \ell n(y_c) + y_c \right) \right. \\ & \qquad \left. + x_\gamma(1-2y_c) \right] \\ & \left. + (1-3\cos^2\theta_\gamma) \left[2\left(\frac{1-x_\gamma}{x_\gamma}\right)\right](2y_c) \right\}. \end{aligned} \tag{54}$$

In Eq. (54), the usual modified minimal subtraction scale is

$$\mu^2_{\overline{\rm MS}} = \mu^2 \; 4\pi \; e^{-\gamma_E}, \tag{55}$$

where γ_E is Euler's constant. The $1/\epsilon$ poles in Eq. (54) arise from the $1/\hat{y}_{13}$ and $1/\hat{y}_{23}$ terms in Eq. (42). Referring to Eq.(21), and using Eqs. (16) and (22), we observe that the $1/\epsilon$ pole in Eq. (54) is exactly canceled. Consequently, for $x_\gamma \le 1/(1+\epsilon_h)$, the finite short-distance hard part is

$$\begin{aligned} E_\gamma \frac{d\hat{\sigma}^{(1)sub}_{e^+e^-\to\gamma X}}{d^3\ell} = & \; 2\sum_q \left[\frac{2}{s} F_q^{PC}(s)\right] \left[\alpha_{em}^2 N_c \frac{1}{x_\gamma}\right] e_q^2 \left(\frac{\alpha_{em}}{2\pi}\right) \\ & \times (1+\cos^2\theta_\gamma) \left\{ \left(\frac{1+(1-x_\gamma)^2}{x_\gamma}\right) \left[\ell n\left(\frac{s}{\mu^2_{\overline{\rm MS}}}\right) + \ell n(x_\gamma^2(1-x_\gamma)) \right. \right. \\ & \qquad \left. \left. + \ell n\left((1-x_\gamma)\frac{\delta^2}{4}\right)\right] + x_\gamma \right\}. \end{aligned} \tag{56}$$

In Eq. (56), we neglect terms of $O(\delta^2)$.

If $x_\gamma > 1/(1+\epsilon_h)$, the negative term, defined through the $\ddot{\otimes}$ convolution in Eq. (21), vanishes. In this region of phase space, there should not be any collinear divergences in the partonic cross section, $E_\gamma d\sigma^{(1)sub}_{e^+e^-\to\gamma X}/d^3\ell$, since there is no counter term to cancel them. If the fragmentation process were exactly collinear, the subtraction term $E_\gamma d\sigma^{(1)sub}_{e^+e^-\to\gamma X}/d^3\ell$

would vanish, kinematically, for $x_\gamma > 1/(1+\epsilon_h)$. However, a finite isolation cone $\delta \neq 0$ allows for a non-vanishing $E_\gamma d\sigma^{(1)sub}_{e^+e^-\to\gamma X}/d^3\ell$ even when $x_\gamma > 1/(1+\epsilon_h)$. Equation (49) shows that there is a narrow interval, $1/(1+\epsilon_h) < x_\gamma < x_\gamma^{\max}(\delta,\epsilon_h)$, in which a non-vanishing $E_\gamma d\sigma^{(1)sub}_{e^+e^-\to\gamma X}/d^3\ell$ is allowed kinematically.

In the narrow interval, $1/(1+\epsilon_h) < x_\gamma < x_\gamma^{\max}(\delta,\epsilon_h)$, the integration over $\hat{y}_{13}$ for $d\sigma^{(1)sub}$ has two separate regions:

$$\int d\hat{y}_{13} \Rightarrow \int_{y_m}^{y_c} d\hat{y}_{13} + \int_{1-y_c}^{1-y_m} d\hat{y}_{13} \ . \tag{57}$$

Equation (48) shows that $y_m > 0$. Therefore, $\hat{y}_{13} > 0$ and $\hat{y}_{13} < 1$. Consequently, there is no collinear divergence and the integration over $\hat{y}_{13}$ can be done completely in $n = 4$ dimensions.

For $1/(1+\epsilon_h) < x_\gamma < x_\gamma^{\max}(\delta,\epsilon_h)$, we derive

$$\begin{aligned}
E_\gamma \frac{d\hat{\sigma}^{(1)sub}_{e^+e^-\to\gamma X}}{d^3\ell} =& \ 2\sum_q \left[\frac{2}{s}F_q^{PC}(s)\right]\left[\alpha_{em}^2 N_c\,\frac{1}{x_\gamma}\right] e_q^2\left(\frac{\alpha_{em}}{2\pi}\right) \\
&\times\Bigg\{(1+\cos^2\theta_\gamma)\left[\left(\frac{1+(1-x_\gamma)^2}{x_\gamma}\right)\left(\ell n\frac{y_c}{y_m}+\ell n\frac{1-y_m}{1-y_c}\right)\right. \\
&\qquad\left. -4x_\gamma\,(y_c-y_m)\right] \\
&\quad +(1-3\cos^2\theta_\gamma)\left[4\left(\frac{1-x_\gamma}{x_\gamma}\right)\right](y_c-y_m)\Bigg\} \\
=& \ 2\sum_q \left[\frac{2}{s}F_q^{PC}(s)\right]\left[\alpha_{em}^2 N_c\,\frac{1}{x_\gamma}\right] e_q^2\left(\frac{\alpha_{em}}{2\pi}\right) \\
&\times(1+\cos^2\theta_\gamma)\left[\left(\frac{1+(1-x_\gamma)^2}{x_\gamma}\right)\ell n\left(\frac{(1-x_\gamma)\delta^2/4}{1+\epsilon_h-1/x_\gamma}\right)\right] \\
&+O(\delta^2).
\end{aligned} \tag{58}$$

We remark that $E_\gamma d\hat{\sigma}^{(1)sub}_{e^+e^-\to\gamma X}/d^3\ell$ in Eq. (58) manifests a logarithmic divergence, of the nature of a collinear divergence, as $x_\gamma \to 1/(1+\epsilon_h)$. This problem arises from the incompatibility of collinear fragmentation, used to define the counter term in Eq. (21), and the cone fragmentation used in the definition of the partonic cross section $E_\gamma d\hat{\sigma}^{(1)sub}_{e^+e^-\to\gamma X}/d^3\ell$ in Eq. (21). More discussion of this issue is presented below, in Sec. IV C.

D. Derivation of $\hat{\sigma}^{(1)sub}_{e^+e^-\to gX}$

In this section we present our explicit expression for the finite short-distance hard part for the order α_s gluon fragmentation process, $e^+e^- \to g \to \gamma$, expressed in Eq.(26). The similarity between the Feynman diagrams for $e^+e^- \to \gamma$, shown in Fig. 5, and those for $e^+e^- \to g \to \gamma$, shown in Fig. 7 allows us to exploit the results derived in the previous subsection.

We derive $\hat{\sigma}^{(1)sub}_{e^+e^-\to gX}$ from the expression for $\hat{\sigma}^{(1)sub}_{e^+e^-\to \gamma X}$, given in Eqs. (56) and (58), by making the following four replacements: $x_\gamma \to x_g$; $N_c \to N_c C_F$; $e^2 e_q^2$ of the final photon emission vertex by $g^2 = 4\pi\alpha_s$; and $\epsilon_h \to \epsilon_{\rm min}(z)$. The last replacement is absent for the inclusive case. Here $z \equiv x_\gamma/x_g$.

If $x_g \le 1/(1+\epsilon_{\rm min})$, which is the same as $x_\gamma \le 1/(1+\epsilon_h)$, these replacements in Eq. (56) provide the finite short-distance hard part

$$\begin{aligned} E_g \frac{d\hat{\sigma}^{(1)sub}_{e^+e^-\to gX}}{d^3p_g} = & \; 2\sum_q \left[\frac{2}{s}F_q^{PC}(s)\right]\left[\alpha_{em}^2 N_c \frac{1}{x_g}\right] C_F\left(\frac{\alpha_s}{2\pi}\right) \\ & \times(1+\cos^2\theta_3)\left\{\left(\frac{1+(1-x_g)^2}{x_g}\right)\left[\ell n\left(\frac{s}{\mu^2_{\overline{\rm MS}}}\right) + \ell n(x_g^2(1-x_g))\right.\right. \\ & \left.\left. + \ell n\left((1-x_g)\frac{\delta^2}{4}\right)\right] + x_g\right\} \\ & + O(\delta^2)\ . \end{aligned} \tag{59}$$

If $x_g > 1/(1+\epsilon_{\rm min})$, which is the same as $x_\gamma > 1/(1+\epsilon_h)$, we make the four replacements in Eq. (58) and find

$$\begin{aligned} E_g \frac{d\hat{\sigma}^{(1)sub}_{e^+e^-\to gX}}{d^3p_g} = & \; 2\sum_q \left[\frac{2}{s}F_q^{PC}(s)\right]\left[\alpha_{em}^2 N_c \, \frac{1}{x_g}\right] C_F\left(\frac{\alpha_s}{2\pi}\right) \\ & \times(1+\cos^2\theta_3)\left[\left(\frac{1+(1-x_g)^2}{x_g}\right)\ell n\left(\frac{(1-x_g)\delta^2/4}{(1+\epsilon_h)(x_\gamma/x_g)-1/x_g}\right)\right] \\ & + O(\delta^2). \end{aligned} \tag{60}$$

From energy-momentum conservation, we derive an equation similar to Eq. (49),

$$E_g \frac{d\hat{\sigma}^{(1)sub}_{e^+e^-\to gX}}{d^3p_g} = 0 \quad \text{if} \quad x_g \ge x^{\rm max}(z,\delta,\epsilon_h). \tag{61}$$

The maximum value $x^{\max}$ is

$$x^{\max}(z,\delta,\epsilon_h) \equiv \left(\frac{1}{z(1+\epsilon_h)}\right) \frac{2}{1+\sqrt{1-\frac{4\sin^2(\delta/2)(z(1+\epsilon_h)-1)}{z^2(1+\epsilon_h)^2}}} \ . \tag{62}$$

The gluon fragmentation contribution to the $O(\alpha_s)$ subtraction term in $\sigma^{(1)sub}_{e^+e^-\to\gamma X}$ is provided by the convolution

$$E_\gamma \frac{d\sigma^{(1)sub}_{e^+e^-\to gX\to\gamma X}}{d^3\ell} = \int_{\max\left[x_\gamma,\frac{1}{1+\epsilon_h}\right]}^1 \frac{dz}{z}\left[E_g \frac{d\hat{\sigma}^{(1)sub}_{e^+e^-\to gX}}{d^3p_g}\left(x_g=\frac{x_\gamma}{z}\right)\right]\frac{D_{g\to\gamma}(z,\mu_F^2)}{z} \ . \tag{63}$$

If collinear fragmentation is assumed for $g\to\gamma$, $\theta_3=\theta_\gamma$. We remark that, after convolution with the gluon-to-photon fragmentation function, the subtraction term $E_g d\hat{\sigma}^{(1)sub}_{e^+e^-\to gX}/d^3p_g$ in Eq. (60) develops a logarithmic divergence $\ell n(1+\epsilon_h-1/x_\gamma)$, as $x_\gamma\to 1/(1+\epsilon_h)$. More discussion of this issue is presented below.

E. Derivation of $\hat{\sigma}^{(1)sub}_{e^+e^-\to qX}$

In this section we evaluate the finite short-distance hard part $\hat{\sigma}^{(1)sub}_{e^+e^-\to qX}$ at order α_s, defined in Eq. (27), for the quark fragmentation process $e^+e^-\to q\to\gamma$. Because $z\geq \max[x_\gamma, 1/(1+\epsilon_h)]$ in the convolutions of Eq. (11), our general analysis of Sec. II shows that the short-distance hard part $\hat{\sigma}^{(1)sub}_{e^+e^-\to qX}$ is needed only for $x_1=x_c\leq \min[x_\gamma(1+\epsilon_h),1]$. We recall that $x_1=2E_q/\sqrt{s}$. We analyze, in turn, the intervals $x_\gamma<1/(1+\epsilon_h)$ and $x_\gamma>1/(1+\epsilon_h)$. Discussion of the special case $x_\gamma=1/(1+\epsilon_h)$ is reserved for Section IV D.

If $x_\gamma<1/(1+\epsilon_h)$, then $x_1<1$ for all values of z in the convolution. In this interval, the virtual diagrams of Fig. 8b, whose contribution is proportional to $\delta(1-x_1)$, do not contribute to $\hat{\sigma}^{(1)sub}_{e^+e^-\to qX}$. The square of the matrix element for $\hat{\sigma}^{(1)sub}_{e^+e^-\to qX}$ is therefore the same as that in Eq. (35), except that the y^2_{ik} variables are no longer those of Eq. (41). Because the quark is now the fragmenting parton, the labels are instead $i=1$, $j=3$, and $h=2$. We obtain

$$
\begin{aligned}
y_{1k}^2 =&\ x_1^2 \cos^2\theta_1; \\
y_{2k}^2 =& \left[\frac{y_{13}y_{23}-y_{12}}{x_1}\right]^2 \cos^2\theta_1 + \frac{1}{1-\epsilon}\left[\frac{2(y_{12}y_{13}y_{23})}{x_1^2}\right]\sin^2\theta_1\ ; \\
y_{3k}^2 =& \left[\frac{y_{12}y_{23}-y_{13}}{x_1}\right]^2 \cos^2\theta_1 + \frac{1}{1-\epsilon}\left[\frac{2(y_{12}y_{13}y_{23})}{x_1^2}\right]\sin^2\theta_1\ .
\end{aligned} \tag{64}
$$

In Eq. (64), θ_1 is the angle between the quark momentum p_1 and the momentum k. In deriving Eq. (64), we dropped terms linear in $\cos\theta_{jx}$, and replaced $\cos^2\theta_{jx}$ by its average in n-dimensions, $1/2(1-\epsilon)$. Substituting these y_{ik}^2 into Eq. (35), and using the identities $y_{23} = 1 - x_1$ and $y_{12} = x_1 - y_{13}$, we derive

$$
\begin{aligned}
\frac{1}{4}\left(H_1 + H_2^{eff}\right) =& (e\mu^\epsilon)^2(g\mu^\epsilon)^2 \left\{ \left(1+\cos^2\theta_1 - 2\epsilon\right)\left[(1-\epsilon)\left(\frac{y_{13}}{y_{23}}+\frac{y_{23}}{y_{13}}\right) + 2\left(\frac{y_{12}}{y_{13}y_{23}} - \epsilon\right)\right]\right. \\
&\left. + \left(1-3\cos^2\theta_1\right)\left[\frac{2y_{12}}{x_1^2}\right]\right\} \\
=& (e\mu^\epsilon)^2(g\mu^\epsilon)^2 \left\{ \left(1+\cos^2\theta_1 - 2\epsilon\right)\left[\left(\frac{1+x_1^2}{1-x_1}\right)\frac{1}{y_{13}} + \frac{y_{13}}{1-x_1}\right]\right. \\
&+ \left(1+\cos^2\theta_1 - 2\epsilon\right)\left[-\frac{2}{1-x_1} - \epsilon\left(\frac{1-x_1}{y_{13}} + \frac{y_{13}}{1-x_1} + 2\right)\right] \\
&\left. + \left(1-3\cos^2\theta_1\right)\left[\frac{2}{x_1}\left(1-\frac{y_{13}}{x_1}\right)\right]\right\}\ .
\end{aligned} \tag{65}
$$

The overall coupling constant $(e\mu^\epsilon)^2(g\mu^\epsilon)^2$ is restored in Eq. (65). Since $x_1 < 1$ for all values of z, there is no infrared divergence associated with $1/(1-x_1)$ terms in Eq. (65).

The isolation condition for the partonic cross section $\sigma^{(1)sub}_{e^+e^-\to qX}$ requires that either the gluon or the antiquark be in the isolation cone of the quark and have energy larger than $E_{\rm min}$ defined in Eq. (8). Following an analysis similar to the one that led to Eq. (47), we derive the limits of the integration over $\hat{y}_{13} \equiv y_{13}/x_1$:

$$
\begin{aligned}
\max[0,\bar{y}_m] \quad &\le \quad \hat{y}_{13} \quad \le \quad \bar{y}_c; \\
1-\bar{y}_c \quad &\le \quad \hat{y}_{13} \quad \le \quad \min[1, 1-\bar{y}_m]\ .
\end{aligned} \tag{66}
$$

In Eq. (66), $\bar{y}_c$ and $\bar{y}_m$ are defined as

$$
\begin{aligned}
\bar{y}_c \equiv& \frac{(1-x_1)\sin^2(\delta/2)}{1-x_1\sin^2(\delta/2)} \quad \Rightarrow \quad (1-x_1)\frac{\delta^2}{4}; \\
\bar{y}_m \equiv& (1+\epsilon_h)z - \frac{1}{x_1};
\end{aligned} \tag{67}
$$

with $z = x_\gamma/x_1$. In analogy to Eq. (61),

$$E_1 \frac{d\hat{\sigma}^{(1)sub}_{e^+e^-\to qX}}{d^3p_1} = 0 \quad \text{if} \quad x_1 \geq x_{\max}(z,\delta,\epsilon_h) \ , \tag{68}$$

where $x_{\max}(z,\delta,\epsilon_h)$ is defined in Eq. (62).

In the region $x_\gamma < 1/(1+\epsilon_h)$, $\bar{y}_m < 0$. The integration over $\hat{y}_{13}$ has two separate intervals:

$$\int d\hat{y}_{13} \Rightarrow \int_0^{\bar{y}_c} d\hat{y}_{13} + \int_{1-\bar{y}_c}^1 d\hat{y}_{13} \ . \tag{69}$$

Integrating over $\hat{y}_{13}$, we obtain

$$\begin{aligned} E_1 \frac{d\sigma^{(1)sub}_{e^+e^-\to qX}}{d^3p_1} = & \left[\frac{2}{s}F_q^{PC}(s)\right]\left[\alpha_{em}^2 N_c \left(\frac{4\pi\mu^2}{(s/4)\sin^2\theta}\right)^\epsilon \frac{1}{\Gamma(1-\epsilon)}\right]\frac{1}{x_1}C_F\left(\frac{\alpha_s}{2\pi}\right) \\ & \times \left\{(1+\cos^2\theta_1 - 2\epsilon)\left(\frac{1+x_1^2}{1-x_1}\right)\left(-\frac{1}{\epsilon}\right)\right. \\ & +(1+\cos^2\theta_1)\left[\left(\frac{1+x_1^2}{1-x_1}\right)\left(\ell n\left(\frac{s}{\mu^2_{\overline{\rm MS}}}\right) + \ell n(x_1^2(1-x_1)) + \ell n\left((1-x_1)\frac{\delta^2}{4}\right)\right)\right. \\ & \left.\left. + (1-x_1)\right]\right\} . \end{aligned} \tag{70}$$

Terms of $O(\delta^2)$ are neglected. The $1/\epsilon$ pole in Eq. (70) arises from the $1/y_{13}$ term in Eq. (65), corresponding to the collinear singularity when the gluon is parallel to the fragmenting quark. Combining Eqs. (16) and Eq. (28), and using the fact that $x_1 < 1$, one may verify that this collinear singularity is canceled exactly by the subtraction term in Eq. (27).

For the finite short-distance subtraction term in the region $x_\gamma < 1/(1+\epsilon_h)$, we obtain

$$\begin{aligned} E_1 \frac{d\hat{\sigma}^{(1)sub}_{e^+e^-\to qX}}{d^3p_1} = & \left[\frac{2}{s}F_q^{PC}(s)\right]\left[\alpha_{em}^2 N_c \ \frac{1}{x_1}\right] C_F\left(\frac{\alpha_s}{2\pi}\right) \\ & \times (1+\cos^2\theta_1)\left\{\left(\frac{1+x_1^2}{1-x_1}\right)\left[\ell n\left(\frac{s}{\mu^2_{\overline{\rm MS}}}\right) + \ell n(x_1^2(1-x_1))\right.\right. \\ & \left.\left. + \ell n\left((1-x_1)\frac{\delta^2}{4}\right)\right] + (1-x_1)\right\} . \end{aligned} \tag{71}$$

Turning to the case $x_1 > 1/(1+\epsilon_{\min(z)})$, which is the same as $x_\gamma > 1/(1+\epsilon_h)$, we note that $\bar{y}_m > 0$. The integration region over $\hat{y}_{13} \equiv y_{13}/x_1$ now has the form

$$\int d\hat{y}_{13} \Rightarrow \int_{\bar{y}_m}^{\bar{y}_c} d\hat{y}_{13} + \int_{1-\bar{y}_c}^{1-\bar{y}_m} d\hat{y}_{13}. \tag{72}$$

Equation (68) shows that $x_1 < 1$ for a nonvanishing $E_1 d\hat{\sigma}^{(1)sub}_{e^+e^-\to qX}/d^3p_1$. Since $x_1 < 1$ and $\hat{y}_{13} \geq \bar{y}_m > 0$, there is neither an infrared nor a collinear divergence in this region. We perform the integration of Eq. (65) over $\hat{y}_{13}$ in $n = 4$ dimensions, and we obtain

$$E_1 \frac{d\hat{\sigma}^{(1)sub}_{e^+e^-\to qX}}{d^3p_1} = \left[\frac{2}{s} F_q^{PC}(s)\right] \left[\alpha_{em}^2 N_c \, \frac{1}{x_1}\right] C_F \left(\frac{\alpha_s}{2\pi}\right) \times (1+\cos^2\theta_1) \left[\left(\frac{1+x_1^2}{1-x_1}\right) \ell n \left(\frac{(1-x_1)\delta^2/4}{(1+\epsilon_h)(x_\gamma/x_1) - 1/x_1}\right)\right] . \quad (73)$$

Terms of $O(\delta^2)$ are dropped. In deriving Eq. (73), we used the fact that the second term in Eq. (27) vanishes in this region.

To summarize the derivation of this subsection, we present a general form for the $O(\alpha_s)$ subtraction term to $\sigma^{(1)sub}_{e^+e^-\to\gamma X}$ via quark fragmentation,

$$E_\gamma \frac{d\sigma^{(1)sub}_{e^+e^-\to qX\to\gamma X}}{d^3\ell} = \sum_q \int_{\max\left[x_\gamma, \frac{1}{1+\epsilon_h}\right]}^1 \frac{dz}{z} \left[E_1 \frac{d\hat{\sigma}^{(1)sub}_{e^+e^-\to qX}}{d^3p_1}\left(x_1 = \frac{x_\gamma}{z}\right)\right] \frac{D_{q\to\gamma}(z,\mu_F^2)}{z} . \quad (74)$$

For collinear fragmentation $q \to \gamma$, $\theta_3 = \theta_\gamma$.

We remark again, as we did in our discussions of the direct and gluon fragmentation contributions, that after convolution with the quark-to-photon fragmentation function, the subtraction term in Eq. (74) manifests a logarithmic divergence of the form $\ell n(1+\epsilon_h - 1/x_\gamma)$ when $x_\gamma \to 1/(1+\epsilon_h)$.

IV. ONE-LOOP CONTRIBUTIONS TO THE ISOLATED CROSS SECTION

Combining the one-loop subtraction terms calculated in last section and the one-loop contributions to the inclusive cross section derived in Ref. [1], we present in this section the complete one-loop contributions to the cross section for isolated photons in e^+e^- collisions.

For the convenience of later discussion, we first list all one-loop contributions to the inclusive cross section, and then we present analytical results for the isolated cross section in three subsections corresponding to $x_\gamma < 1/(1+\epsilon_h)$, $x_\gamma > 1/(1+\epsilon_h)$, and $x_\gamma = 1/(1+\epsilon_h)$, respectively. We conclude this section with a discussion of the logarithmic divergence associated with the special point $x_\gamma \Rightarrow 1/(1+\epsilon_h)$.

A. One-Loop Contributions to the Inclusive Cross Section

Complete one-loop contributions to the inclusive cross section, $E_\gamma d\sigma^{incl}_{e^+e^-\to\gamma X}/d^3\ell$, are derived in Ref. [1]. The results are summarized as follows.

One-loop direct production of $e^+e^- \to \gamma$ at $O(\alpha_{em})$:

$$E_\gamma \frac{d\hat{\sigma}^{(1)incl}_{e^+e^-\to\gamma X}}{d^3\ell} = 2\sum_q \left[\frac{2}{s}F_q^{PC}(s)\right]\left[\alpha_{em}^2 N_c \frac{1}{x_\gamma}\right] e_q^2 \left(\frac{\alpha_{em}}{2\pi}\right) \times \left\{(1+\cos^2\theta_\gamma)\left(\frac{1+(1-x_\gamma)^2}{x_\gamma}\right)\left[\ell n\left(\frac{s}{\mu^2_{\overline{\rm MS}}}\right) + \ell n(x_\gamma^2(1-x_\gamma))\right] + (1-3\cos^2\theta_\gamma)\left[\frac{2(1-x_\gamma)}{x_\gamma}\right]\right\}. \tag{75}$$

One-loop fragmentation contribution via a gluon: $e^+e^- \to g \to \gamma$ at $O(\alpha_s)$:

$$E_\gamma \frac{d\sigma^{(1)incl}_{e^+e^-\to gX\to\gamma X}}{d^3\ell} = \int_{x_\gamma}^1 \frac{dz}{z}\left[E_g \frac{d\hat{\sigma}^{(1)incl}_{e^+e^-\to gX}}{d^3p_g}\left(x_g = \frac{x_\gamma}{z}\right)\right]\frac{D_{g\to\gamma}(z,\mu_F^2)}{z}, \tag{76}$$

where the short-distance hard part is

$$E_g \frac{d\hat{\sigma}^{(1)incl}_{e^+e^-\to gX}}{d^3p_g} = 2\sum_q \left[\frac{2}{s}F_q^{PC}(s)\right]\left[\alpha_{em}^2 N_c \frac{1}{x_g}\right] C_F \left(\frac{\alpha_s}{2\pi}\right) \times \left\{(1+\cos^2\theta_\gamma)\left(\frac{1+(1-x_g)^2}{x_g}\right)\left[\ell n\left(\frac{s}{\mu^2_{\overline{\rm MS}}}\right) + \ell n(x_g^2(1-x_g))\right] + (1-3\cos^2\theta_\gamma)\left[\frac{2(1-x_g)}{x_g}\right]\right\}, \tag{77}$$

with $x_g = 2E_g/\sqrt{s}$, and $\theta_g = \theta_\gamma$.

One-loop fragmentation contribution through a quark, $e^+e^- \to q \to \gamma$ at $O(\alpha_s)$:

$$E_\gamma \frac{d\sigma^{(1)incl}_{e^+e^-\to qX\to\gamma X}}{d^3\ell} = \sum_q \int_{x_\gamma}^1 \frac{dz}{z}\left[E_1 \frac{d\hat{\sigma}^{(1)incl}_{e^+e^-\to qX}}{d^3p_1}\left(x_1 = \frac{x_\gamma}{z}\right)\right]\frac{D_{q\to\gamma}(z,\mu_F^2)}{z}, \tag{78}$$

where the short-distance hard part is

$$E_1 \frac{d\hat{\sigma}^{(1)incl}_{e^+e^-\to qX}}{d^3p_1} = \left[\frac{2}{s}F_q^{PC}(s)\right]\left[\alpha_{em}^2 N_c \frac{1}{x_1}\right] C_F \left(\frac{\alpha_s}{2\pi}\right) \times \left\{(1+\cos^2\theta_\gamma)\left[\left(\frac{1+x_1^2}{(1-x_1)_+} + \frac{3}{2}\delta(1-x_1)\right)\ell n\left(\frac{s}{\mu^2_{\overline{\rm MS}}}\right) + \left(\frac{1+x_1^2}{1-x_1}\right)\ell n\left(x_1^2\right) + \left(1+x_1^2\right)\left(\frac{\ell n(1-x_1)}{1-x_1}\right)_+ - \frac{3}{2}\left(\frac{1}{1-x_1}\right)_+\right.$$

$$+\delta(1-x_1)\left(\frac{2\pi^2}{3}-\frac{9}{2}\right)-\frac{1}{2}\left(3x_1-5\right)\Bigg]$$
$$+\left(1-3\cos^2\theta_\gamma\right)\Bigg\}\,. \tag{79}$$

Here $\theta_1=\theta_\gamma$ is used, and the "+" description is defined in Eq. (29).

B. One-Loop Contribution to the Isolated Cross Section when $x_\gamma < 1/(1+\epsilon_h)$

Substituting Eqs. (56) and (75) into Eq. (13a) for $c=\gamma$, we derive the $O(\alpha_{em})$ one-loop direct production of isolated photons via $e^+e^-\to\gamma$:

$$\begin{aligned}E_\gamma\frac{d\hat{\sigma}^{(1)iso}_{e^+e^-\to\gamma X}}{d^3\ell} =\; & 2\sum_q\left[\frac{2}{s}F_q^{PC}(s)\right]\left[\alpha_{em}^2N_c\frac{1}{x_\gamma}\right]e_q^2\left(\frac{\alpha_{em}}{2\pi}\right)\\ &\times\Bigg\{(1+\cos^2\theta_\gamma)\left[\left(\frac{1+(1-x_\gamma)^2}{x_\gamma}\right)\ell n\left(\frac{1}{(1-x_\gamma)\delta^2/4}\right)-x_\gamma\right]\\ &+(1-3\cos^2\theta_\gamma)\left[\frac{2(1-x_\gamma)}{x_\gamma}\right]\Bigg\}\,,\end{aligned} \tag{80}$$

where we have dropped terms of $O(\delta^2)$. By integrating over θ_γ, we may verify that Eq. (80) is consistent with the analogous expression derived in Ref. [3].

From Eqs. (11), (59) and (77), we obtain the $O(\alpha_s)$ one-loop gluonic fragmentation contribution to the cross section for isolated photons:

$$E_\gamma\frac{d\sigma^{(1)iso}_{e^+e^-\to gX\to\gamma X}}{d^3\ell}=\int_{\max\left[x_\gamma,\frac{1}{1+\epsilon_h}\right]}^1\frac{dz}{z}\left[E_g\frac{d\hat{\sigma}^{(1)iso}_{e^+e^-\to gX}}{d^3p_g}\left(x_g=\frac{x_\gamma}{z}\right)\right]\frac{D_{g\to\gamma}(z,\mu_F^2)}{z}\,, \tag{81}$$

where the short-distance hard part is

$$\begin{aligned}E_g\frac{d\hat{\sigma}^{(1)iso}_{e^+e^-\to gX}}{d^3p_g} =\; & 2\sum_q\left[\frac{2}{s}F_q^{PC}(s)\right]\left[\alpha_{em}^2N_c\frac{1}{x_g}\right]C_F\left(\frac{\alpha_s}{2\pi}\right)\\ &\times\Bigg\{(1+\cos^2\theta_\gamma)\left[\left(\frac{1+(1-x_g)^2}{x_g}\right)\ell n\left(\frac{1}{(1-x_g)\delta^2/4}\right)-x_g\right]\\ &+(1-3\cos^2\theta_\gamma)\left[\frac{2(1-x_g)}{x_g}\right]\Bigg\}\,.\end{aligned} \tag{82}$$

Similarly, we derive the $O(\alpha_s)$ one-loop quark fragmentation contribution to the cross section for isolated photons:

$$E_\gamma \frac{d\sigma^{(1)iso}_{e^+e^-\to qX\to\gamma X}}{d^3\ell} = \sum_q \int_{\max\left[x_\gamma,\frac{1}{1+\epsilon_h}\right]}^1 \frac{dz}{z}\left[E_1 \frac{d\hat{\sigma}^{(1)iso}_{e^+e^-\to qX}}{d^3p_1}\left(x_1=\frac{x_\gamma}{z}\right)\right]\frac{D_{q\to\gamma}(z,\mu_F^2)}{z}\,, \quad (83)$$

where the short-distance hard part is

$$\begin{aligned} E_q \frac{d\hat{\sigma}^{(1)iso}_{e^+e^-\to qX}}{d^3p_q} = & \left[\frac{2}{s}F_q^{PC}(s)\right]\left[\alpha_{em}^2 N_c \frac{1}{x_1}\right] C_F \left(\frac{\alpha_s}{2\pi}\right) \\ & \times \left\{ \left(1+\cos^2\theta_\gamma\right)\left[\left(\frac{1+x_1^2}{1-x_1}\right)\ell n\left(\frac{1}{(1-x_1)\delta^2/4}\right) - \frac{3}{2}\left(\frac{1}{1-x_1}\right) - \frac{1}{2}\left(x_1-3\right)\right] \right. \\ & \left. + \left(1-3\cos^2\theta_\gamma\right)\right\}\,. \end{aligned} \quad (84)$$

Equation (84) is derived by substituting Eqs. (71) and (79) into Eq. (13b). We observe after integrating over z, that Eq. (83) develops a logarithmic divergence $\ell n(1/x_\gamma - (1+\epsilon_h))$ as $x_\gamma \to 1/(1+\epsilon_h)$. This divergence is caused by the $1/(1-x_1)$ terms in Eq. (84). A detailed discussion of this divergence is presented later in subsection IV D.

Assuming $D_{q\to\gamma}(z) = D_{\bar{q}\to\gamma}(z)$, the one-loop antiquark fragmentation contribution to the cross section for isolated photons is the same as that of the quark contribution in Eq. (83), except that the $\sum$ is over $\bar{q}$.

C. One-Loop Contribution to the Isolated Cross Section when $x_\gamma > 1/(1+\epsilon_h)$

As pointed out in Section III, the subtraction terms $\hat{\sigma}^{(1)sub}$ would vanish for $x_\gamma > 1/(1+\epsilon_h)$ if all fragmentation processes were exactly collinear. But, due to the finite cone size, there is a small region of phase space where the subtraction terms are finite. Since the value of ϵ_h is very small in most experiments, very limited data from $e^+e^- \to \gamma X$ are available in this region. Nevertheless, the isolated cross section in this region is interesting theoretically and important for understanding the isolated cross section in hadron-hadron collisions.

Kinematics require the subtraction term $E_\gamma d\hat{\sigma}^{(1)sub}_{e^+e^-\to\gamma X}/d^3\ell$ to vanish if $x_\gamma > x_\gamma^{\max}(\delta,\epsilon_h)$, defined in Eq. (50); therefore,

$$E_\gamma \frac{d\hat{\sigma}^{(1)iso}_{e^+e^-\to\gamma X}}{d^3\ell} = E_\gamma \frac{d\hat{\sigma}^{(1)incl}_{e^+e^-\to\gamma X}}{d^3\ell} \qquad \text{if } x_\gamma > x_\gamma^{\max}(\delta,\epsilon_h). \quad (85)$$

However, if $1/(1+\epsilon_h) < x_\gamma < x_\gamma^{\max}(\delta,\epsilon_h)$, we use Eqs. (58) and (75) to derive

$$E_\gamma \frac{d\hat{\sigma}^{(1)iso}_{e^+e^-\to\gamma X}}{d^3\ell} = 2\sum_q \left[\frac{2}{s}F_q^{PC}(s)\right]\left[\alpha_{em}^2 N_c \frac{1}{x_\gamma}\right] e_q^2 \left(\frac{\alpha_{em}}{2\pi}\right)$$
$$\times \left\{ \left(1+\cos^2\theta_\gamma\right)\left(\frac{1+(1-x_\gamma)^2}{x_\gamma}\right)\left[\ell n\left(\frac{s}{\mu^2_{\overline{\rm MS}}}\right) + \ell n(x_\gamma^2(1-x_\gamma)) \right.\right.$$
$$\left. + \ell n\left(\frac{1+\epsilon_h - 1/x_\gamma}{(1-x_\gamma)\delta^2/4}\right)\right]$$
$$\left. + \left(1-3\cos^2\theta_\gamma\right)\left[\frac{2(1-x_\gamma)}{x_\gamma}\right]\right\}. \tag{86}$$

If we integrate Eq. (86) over θ_γ, we obtain the analogous result derived previously in Ref. [3].

For the one-loop fragmentation contributions from parton $c(= g, q, \bar{q})$ to γ, the subtraction terms again vanish if $x_c > x^{\max}(z,\delta,\epsilon_h)$, defined in Eq. (62); thus,

$$E_c \frac{d\hat{\sigma}^{(1)iso}_{e^+e^-\to cX}}{d^3p_c} = E_c \frac{d\hat{\sigma}^{(1)incl}_{e^+e^-\to cX}}{d^3p_c} \qquad \text{if } x_c > x^{\max}(z,\delta,\epsilon_h)\ . \tag{87}$$

In Eq. (87), the corresponding inclusive hard parts are given in Eqs. (77) and (79).

If $1/(1+\epsilon_h) < x_c < x^{\max}(z,\delta,\epsilon_h)$, the subtraction terms are finite and are given in Eqs. (60) and (73). Combining Eq. (60) with the inclusive contribution, we obtain the gluon fragmentation contribution as

$$E_g \frac{d\hat{\sigma}^{(1)iso}_{e^+e^-\to gX}}{d^3p_g} = 2\sum_q \left[\frac{2}{s}F_q^{PC}(s)\right]\left[\alpha_{em}^2 N_c \frac{1}{x_g}\right] C_F\left(\frac{\alpha_s}{2\pi}\right)$$
$$\times \left\{ (1+\cos^2\theta_\gamma)\left(\frac{1+(1-x_g)^2}{x_g}\right)\left[\ell n\left(\frac{s}{\mu^2_{\overline{\rm MS}}}\right) + \ell n(x_g^2(1-x_g)) \right.\right.$$
$$\left. + \ell n\left(\frac{(1+\epsilon_h)(x_\gamma/x_g) - 1/x_g}{(1-x_g)\delta^2/4}\right)\right]$$
$$\left. + (1-3\cos^2\theta_\gamma)\left[\frac{2(1-x_g)}{x_g}\right]\right\} \tag{88}$$

for $1/(1+\epsilon_h) < x_g < x^{\max}(z,\delta,\epsilon_h)$. The quark fragmentation contribution is

$$E_q \frac{d\hat{\sigma}^{(1)iso}_{e^+e^-\to qX}}{d^3p_q} = \left[\frac{2}{s}F_q^{PC}(s)\right]\left[\alpha_{em}^2 N_c \frac{1}{x_1}\right] C_F\left(\frac{\alpha_s}{2\pi}\right)$$
$$\times \left\{ (1+\cos^2\theta_\gamma)\left[\left(\frac{1+x_1^2}{1-x_1}\right)\left[\ell n\left(\frac{s}{\mu^2_{\overline{\rm MS}}}\right) + \ell n\left(x_1^2(1-x_1)\right)\right.\right.\right.$$
$$\left.\left. + \ell n\left(\frac{(1+\epsilon_h)(x_\gamma/x_1) - 1/x_1}{(1-x_1)\delta^2/4}\right)\right] - \frac{3}{2}\left(\frac{1}{1-x_1}\right) - \frac{1}{2}(3x_1-5)\right]$$
$$\left. + \left(1-3\cos^2\theta_\gamma\right)\right\} \tag{89}$$

for $1/(1+\epsilon_h) < x_1 < x^{\max}(z,\delta,\epsilon_h)$; $x^{\max}(z,\delta,\epsilon_h)$ is defined in Eq. (62).

It is a common feature of Eqs. (86), (88) and (89) that all three develop a logarithmic divergence $\ell n(1+\epsilon_h - 1/x_\gamma)$ as $x_\gamma \to 1/(1+\epsilon_h)$. This logarithm results from the collinear singularities of the Feynman diagrams shown in Figs. 5, 7 and 8a. It corresponds to the situation in which an unobserved parton inside the isolation cone becomes almost collinear with the observed parton. Since $x_\gamma > 1/(1+\epsilon_h)$, which is the same as x_g or $x_q > 1/(1+\epsilon_{\min}(z))$ for all z, the counter terms, defined through $\ddot{\otimes}$ in Eqs. (21), (26), and (27), vanish. Consequently, the collinear singularities have no corresponding canceling counter terms.

This problem is caused by the incompatibility between collinear fragmentation, which was used to define the counter terms in Eqs. (21), (26) and (27), and the cone fragmentation used to define the partonic cross section $E_\gamma d\hat{\sigma}^{(1)sub}_{e^+e^-\to cX}/d^3\ell$ with $c = \gamma, q, \bar{q}, g$ in Eqs. (21) (26), and (27). As we pointed out in Section I, to deal with the region $x_\gamma > 1/(1+\epsilon_h)$ it may be necessary to revise our concept of photon fragmentation functions in the case of isolated photons.

D. One-Loop Contribution to the Isolated Cross Section when $x_\gamma = 1/(1+\epsilon_h)$

As x_γ approaches $1/(1+\epsilon_h)$, a number of the expressions derived above for the isolated cross section develop a logarithmic divergence of the form $\ell n|(1+\epsilon_h) - 1/x_\gamma|$. However, the value of ϵ_h is an arbitrary parameter chosen in individual experiments. Certainly, a completely consistent theoretical prediction should not be sensitive to an arbitrary experimental parameter, such as ϵ_h. We argue below that the reason for the unstable result as x_γ approaches $1/(1+\epsilon_h)$ is the breakdown [5] of the conventional perturbative factorization theorem for the cross section of isolated photons in the neighborhood of $x_\gamma = 1/(1+\epsilon_h)$.

In this subsection, we first use our results of the last two subsections to explain the origin of this logarithmic divergence. Then, we present a derivation of the isolated cross section for x_γ near the value $1/(1+\epsilon_h)$, and we show that the key issues are the isolation condition and the finite cone size for fragmentation.

We start with the situation in which x_γ approaches $1/(1+\epsilon_h)$ from below. When x_γ is less than $1/(1+\epsilon_h)$, the expression for direct production, given in Eq. (80), is well-behaved as x_γ approaches $1/(1+\epsilon_h)$. Similarly, the gluonic fragmentation contribution, defined by Eqs. (81) and (82), is also well-behaved as x_γ approaches $1/(1+\epsilon_h)$. Although x_g can equal 1 when $x_\gamma = 1/(1+\epsilon_h)$, the $\ell n(1-x_g)$ term in Eq. (82) gives a finite contribution after the integration over z. Thus, Eqs. (80) and (81) should also be valid at $x_\gamma = 1/(1+\epsilon_h)$.

On the other hand, the quark (or antiquark) fragmentation contribution develops a logarithmic divergence as x_γ approaches $1/(1+\epsilon_h)$. This divergence is caused by the $1/(1-x_1)$ terms in Eq. (84), and it can be understood as follows. Consider the following general integral

$$I(x_\gamma,\epsilon_h) \equiv \int_{1/(1+\epsilon_h)}^{1} \frac{dz}{z}\left(\frac{1}{1-x_1}\right)\ell n^m(1-x_1)F(z,x_1=x_\gamma/z), \qquad \text{for } x_\gamma \le 1/(1+\epsilon_h), \tag{90}$$

where $m = 0, 1, ...$, and $F(z, x_1 = x_\gamma/z)$ is any smooth function over the region of integration. The integral $I(x_\gamma, \epsilon_h)$ can be thought of as a simplified version of the one-loop quark fragmentation contribution defined in Eq. (83). The factors $1/(1-x_1)$ and $\ell n(1-x_1)$ are typical of the short-distance hard part. It is straightforward to perform the integration, and we find

$$\begin{aligned} I(x_\gamma,\epsilon_h) \;&=\; \int_{x_\gamma}^{x_\gamma(1+\epsilon_h)} \frac{dx_1}{x_1}\left(\frac{1}{1-x_1}\right)\ell n^m(1-x_1)F(z=x_\gamma/x_1,x_1) \\ &\Rightarrow -\ell n^{m+1}\left(1-x_\gamma(1+\epsilon_h)\right) \quad \Rightarrow \pm\infty \qquad \text{as } x_\gamma \to 1/(1+\epsilon_h). \end{aligned} \tag{91}$$

This example shows that $1/(1-x_1)$ terms in the short-distance hard part make the isolated cross section very sensitive to the value of ϵ_h, as x_γ approaches $1/(1+\epsilon_h)$. The perturbatively calculated cross section for isolated photons becomes logarithmically divergent at a different value of x_γ if one chooses a different value of ϵ_h.

The reason for this unsatisfactory logarithmic sensitivity is the infrared divergence associated with the limit in which the final-state gluon's momentum goes to zero, which is the same as $x_1 \to 1$. Normally, such an infrared divergence is canceled by virtual diagrams. For

example, in the calculation of the inclusive contribution, the infrared singularity associated with $x_1 \to 1$ from the real gluon emission diagrams, sketched in Fig. 8a, is canceled by the infrared contribution from the virtual gluon exchange diagrams, sketched in Fig. 8b, proportional to $\delta(1-x_1)$. However, as we demonstrate below, perfect cancellation between real and virtual diagrams is upset by the isolation conditions.

Isolated photons are defined to be photons accompanied by less than $E_{max} = \epsilon_h E_\gamma$ of hadronic energy in the isolation cone. For photons produced from parton fragmentation, as sketched in Fig. 3, a situation can arise in which E_{max} in the isolation cone is provided completely by parton fragmentation. Consequently, no other soft gluons are allowed to enter the isolation cone. The phase space for the final-state non-fragmenting partons is reduced by the size of the cone. Due to the mismatch of the phase space, the infrared divergences associated with the final-state real gluons cannot be completely canceled by the virtual diagrams. Such uncanceled infrared contributions vanish if the cone size is zero.

As an example, we use the one-loop quark fragmentation contribution to the cross section for isolated photons to demonstrate the breakdown of the perfect cancellation of infrared divergences. In order to make our presentation parallel the statements of the last paragraph, we calculate the isolated cross section from the quark fragmentation term directly without going through the subtraction term [5].

To examine the situation in which x_γ approaches $1/(1+\epsilon_h)$, we must evaluate both the real and the virtual diagrams shown in Fig. 8. The squared matrix element for the real diagrams is obtained from Eq. (65):

$$\begin{aligned}
\frac{1}{4}H^{real} &= \frac{1}{4}\left(H_1 + H_2^{eff}\right) \\
&= (e\mu^\epsilon)^2(g\mu^\epsilon)^2\Bigg\{\left(1+\cos^2\theta_1 - 2\epsilon\right)\left[\left(\frac{1+x_1^2}{1-x_1}\right)\frac{1}{y_{13}} + \frac{y_{13}}{1-x_1}\right] \\
&\quad + \left(1+\cos^2\theta_1 - 2\epsilon\right)\left[-\frac{2}{1-x_1} - \epsilon\left(\frac{1-x_1}{y_{13}} + \frac{y_{13}}{1-x_1} + 2\right)\right] \\
&\quad + \left(1-3\cos^2\theta_1\right)\left[\frac{2}{x_1}\left(1-\frac{y_{13}}{x_1}\right)\right]\Bigg\}\,. \qquad (92)
\end{aligned}$$

Equation (92) holds for both the inclusive and the isolated cross sections. The key difference

resides in the limits of integration over $\hat{y}_{13} = y_{13}/x_1$. Integrating $\hat{y}_{13}$ from 0 to 1, we obtain the real contribution to the inclusive cross section; all infrared divergences associated with $x_1 \to 1$ are canceled by the contribution from the virtual diagrams [1]. On the other hand, the isolation conditions require that the $\hat{y}_{13}$ integration be divided into three regions:

$$\int d\hat{y}_{13} \Rightarrow \int_0^{\min[\bar{y}_c,\bar{y}_m]} d\hat{y}_{13} + \int_{\bar{y}_c}^{1-\bar{y}_c} d\hat{y}_{13} + \int_{\max[(1-\bar{y}_c),(1-\bar{y}_m)]}^{1} d\hat{y}_{13} \ , \tag{93}$$

where $\bar{y}_c$ and $\bar{y}_m$ are defined in Eq. (67). In the first region, the condition $0 \leq \hat{y}_{13} \leq \bar{y}_c$ ensures that a gluon is in the isolation cone of the fragmenting quark; and condition $\hat{y}_{13} \leq \min[\bar{y}_c, \bar{y}_m]$ ensures that the total hadronic energy in the isolation cone is less than $E_{max} = \epsilon_h E_\gamma$. Similarly, the condition $\max[(1-\bar{y}_c), (1-\bar{y}_m)] \leq \hat{y}_{13} \leq 1$ for the third region ensures that the antiquark is in the isolation cone and that the total hadronic energy in the isolation cone is less than E_{max}. The second interval represents the situation in which neither the gluon nor the antiquark is in the isolation cone.

If $\bar{y}_c \leq \bar{y}_m$, Eq. (93) shows that the isolated cross section is the same as the inclusive cross section, consistent with Eq. (68). When $\bar{y}_c > \bar{y}_m$, (i.e., $(1-x_1)\delta^2/4 > z[(1+\epsilon_h) - 1/x_\gamma]$), Eq. (93) states that the phase space of the final state gluon (and/or antiquark) is <u>smaller</u> than in the case of the inclusive cross section.

If $x_\gamma \leq 1/(1+\epsilon_h)$, or, equivalently, $\bar{y}_m = z[(1+\epsilon_h) - 1/x_\gamma] \leq 0$, the $\hat{y}_{13}$ integration defined in Eq. (93) reduces to the second region only

$$\int d\hat{y}_{13} \Rightarrow \int_{(1-x_1)\delta^2/4}^{1-(1-x_1)\delta^2/4} d\hat{y}_{13}, \tag{94}$$

where we expand $\bar{y}_c$ to order δ^2. We rewrite the limits of the integration over $\hat{y}_{13}$ in Eq. (94) as

$$\int_{(1-x_1)\delta^2/4}^{1-(1-x_1)\delta^2/4} d\hat{y}_{13} = \int_0^1 d\hat{y}_{13} - \int_0^{(1-x_1)\delta^2/4} d\hat{y}_{13} - \int_{1-(1-x_1)\delta^2/4}^1 d\hat{y}_{13}. \tag{95}$$

Combining the three-particle phase space of Eq. (33) and the squared matrix element of Eq. (92), we derive that the <u>first</u> term on the right-hand-side of Eq. (95) provides the complete real gluon emission contribution for the inclusive cross section [1]

$$
\begin{aligned}
E_1\frac{d\sigma^{(R_1)}_{e^+e^-\to qX}}{d^3p_1} &= \left[\frac{2}{s}\,F^{PC}(s)\right]\left[\alpha_{em}^2\,N_c\left(\frac{4\pi\mu^2}{(s/4)\sin^2\theta_1}\right)^{\epsilon}\frac{1}{\Gamma(1-\epsilon)}\,\frac{1}{x_1}\right] \\
&\times C_F\left(\frac{\alpha_s}{2\pi}\right)\left[\left(\frac{4\pi\mu^2}{s}\right)^{\epsilon}\frac{1}{\Gamma(1-\epsilon)}\right]\frac{\Gamma(1-\epsilon)^2}{\Gamma(1-2\epsilon)} \\
&\times\left\{\left(1+\cos^2\theta_1-2\epsilon\right)\left[\left(\frac{1+x_1^2}{(1-x_1)_+}+\frac{3}{2}\delta(1-x_1)\right)\left(\frac{1}{-\epsilon}\right)\right.\right. \\
&\qquad +\left(\frac{1+x_1^2}{1-x_1}\right)\ell n\left(x_1^2\right)+\left(1+x_1^2\right)\left(\frac{\ell n(1-x_1)}{1-x_1}\right)_+-\frac{3}{2}\left(\frac{1}{1-x_1}\right)_+ \\
&\qquad \left.+\delta(1-x_1)\left(\frac{2}{\epsilon^2}+\frac{3}{\epsilon}+\frac{7}{2}\right)-\frac{1}{2}\left(3x_1-5\right)\right] \\
&\left.+\left(1-3\cos^2\theta_1\right)\right\}. \qquad (96)
\end{aligned}
$$

The superscript (R_1) stands for the contribution of real gluon emission from the first term on the right-hand-side of Eq. (95). In deriving Eq. (96), we use

$$
\frac{1}{(1-x_1)^{1+\epsilon}}=-\frac{1}{\epsilon}\delta(1-x_1)+\left(\frac{1}{1-x_1}\right)_+-\epsilon\left(\frac{\ell n(1-x_1)}{1-x_1}\right)_+. \qquad (97)
$$

The virtual gluon exchange contribution from the diagrams in Fig. 8b is [1]

$$
\begin{aligned}
E_1\frac{d\sigma^{(V)}_{e^+e^-\to qX}}{d^3p_1} &= \left[\frac{2}{s}\,F^{PC}(s)\right]\left[\alpha_{em}^2\,N_c\left(\frac{4\pi\mu^2}{(s/4)\sin^2\theta_1}\right)^{\epsilon}\frac{1}{\Gamma(1-\epsilon)}\,\frac{1}{x_1}\right] \\
&\times C_F\left(\frac{\alpha_s}{2\pi}\right)\left[\left(\frac{4\pi\mu^2}{s}\right)^{\epsilon}\frac{1}{\Gamma(1-\epsilon)}\right]\frac{\Gamma(1-\epsilon)^3\Gamma(1+\epsilon)}{\Gamma(1-2\epsilon)} \\
&\times\left\{\left(1+\cos^2\theta_1-2\epsilon\right)\delta(1-x_1)\left[-\frac{2}{\epsilon^2}-\frac{3}{\epsilon}+\left(\pi^2-8\right)\right]\right\}, \qquad (98)
\end{aligned}
$$

where the superscript (V) stands for the virtual gluon exchange contribution.

Combining the virtual (V) contribution and a part of the real contribution (R_1), we derive

$$
\begin{aligned}
E_1\frac{d\sigma^{(R_1+V)}_{e^+e^-\to qX}}{d^3p_1} &= \left[\frac{2}{s}\,F^{PC}(s)\right]\left[\alpha_{em}^2\,N_c\left(\frac{4\pi\mu^2}{(s/4)\sin^2\theta_1}\right)^{\epsilon}\frac{1}{\Gamma(1-\epsilon)}\frac{1}{x_1}\right] \\
&\times C_F\left(\frac{\alpha_s(\mu^2)}{2\pi}\right)\left\{\left(1+\cos^2\theta_1-2\epsilon\right)\left[\frac{1+x_1^2}{(1-x_1)_+}+\frac{3}{2}\delta(1-x_1)\right]\left(\frac{1}{-\epsilon}\right)\right\} \\
&+\left[\frac{2}{s}\,F^{PC}(s)\right]\left[\alpha_{em}^2\,N_c\,\frac{1}{x_1}\right]C_F\left(\frac{\alpha_s(\mu^2)}{2\pi}\right) \\
&\times\left\{(1+\cos^2\theta_1)\left[\left(\frac{1+x_1^2}{(1-x_1)_+}+\frac{3}{2}\delta(1-x_1)\right)\ell n\left(\frac{s}{\mu^2_{\overline{\rm MS}}}\right)\right.\right.
\end{aligned}
$$

$$+\left(\frac{1+x_1^2}{1-x_1}\right)\ell n\left(x_1^2\right)+\left(1+x_1^2\right)\left(\frac{\ell n(1-x_1)}{1-x_1}\right)_+-\frac{3}{2}\left(\frac{1}{1-x_1}\right)_+$$
$$+\delta(1-x_1)\left(\frac{2\pi^2}{3}-\frac{9}{2}\right)-\frac{1}{2}\left(3x_1-5\right)\Bigg]$$
$$+\left(1-3\cos^2\theta_1\right)\Bigg\}\,. \tag{99}$$

As expected, Eq. (99) shows that, except for the $1/\epsilon$ term associated with the collinear singularity between the fragmenting quark and the real gluon, the contribution from the first term on the right-hand-side of Eq. (95) cancels all infrared singularities from the virtual diagrams in Fig. 8b.

The third term in Eq. (95) does not provide any terms singular in $1/\epsilon$; it yields some finite terms that vanish as $\delta^2 \to 0$,

$$E_1\frac{d\sigma^{(R_3)}_{e^+e^-\to qX}}{d^3p_1}=O(\delta^2)\,. \tag{100}$$

However, the second term generates a number of terms with $1/\epsilon$ poles. Neglecting all terms of $O(\delta^2)$ or higher, we obtain

$$\begin{aligned}
E_1\frac{d\sigma^{(R_2)}_{e^+e^-\to qX}}{d^3p_1} =& -\left[\frac{2}{s}F^{PC}(s)\right]\left[\alpha_{em}^2\,N_c\left(\frac{4\pi\mu^2}{(s/4)\sin^2\theta_1}\right)^{\epsilon}\frac{1}{\Gamma(1-\epsilon)}\frac{1}{x_1}\right]\\
&\times C_F\left(\frac{\alpha_s(\mu^2)}{2\pi}\right)\left\{\left(1+\cos^2\theta_1-2\epsilon\right)\left[\frac{1+x_1^2}{(1-x_1)_+}+\frac{3}{2}\delta(1-x_1)\right]\left(\frac{1}{-\epsilon}\right)\right\}\\
-&\left[\frac{2}{s}F^{PC}(s)\right]\left[\alpha_{em}^2\,N_c\,\frac{1}{x_1}\right]C_F\left(\frac{\alpha_s(\mu^2)}{2\pi}\right)\\
&\times\left(1+\cos^2\theta_1\right)\Bigg[\left(\frac{1+x_1^2}{(1-x_1)_+}+\frac{3}{2}\delta(1-x_1)\right)\ell n\left(\frac{s}{\mu^2_{\overline{\rm MS}}}\right)\\
&\quad+\frac{1+x_1^2}{1-x_1}\ell n\left(x_1^2\right)+2\left(1+x_1^2\right)\left(\frac{\ell n(1-x_1)}{1-x_1}\right)_+-\frac{1+x_1^2}{(1-x_1)_+}\ell n\frac{\delta^2}{4}\\
&\quad+\delta(1-x_1)\,\ell n^2\frac{\delta^2}{4}+(1-x_1)\Bigg]\\
-&\left[\frac{2}{s}F^{PC}(s)\right]\left[\alpha_{em}^2\,N_c\left(\frac{4\pi\mu^2}{(s/4)\sin^2\theta_1}\right)^{\epsilon}\frac{1}{\Gamma(1-\epsilon)}\,\frac{1}{x_1}\right]\\
&\times\left(1+\cos^2\theta_1-2\epsilon\right)C_F\left(\frac{\alpha_s(\mu^2)}{2\pi}\right)\left[\left(\frac{4\pi\mu^2}{s}\right)^{\epsilon}\frac{1}{\Gamma(1-\epsilon)}\right]\\
&\times\left[\frac{1}{\epsilon^2}+\frac{1}{\epsilon}\left(\frac{3}{2}-\ell n\frac{\delta^2}{4}\right)\right]\delta(1-x_1)\,.
\end{aligned} \tag{101}$$

Collecting the contributions in Eqs. (99), (100), and (101), we find the complete next-to-leading order isolated partonic cross section for $e^+ + e^- \to q(p_1) + X$,

$$
\begin{aligned}
E_1 \frac{d\sigma^{(1)iso}_{e^+e^-\to qX}}{d^3p_1} &= E_1 \frac{d\sigma^{(R+V)}_{e^+e^-\to qX}}{d^3p_1} \\
&= \left[\frac{2}{s}\, F^{PC}(s)\right]\left[\alpha_{em}^2\, N_c\, \frac{1}{x_1}\right] C_F \left(\frac{\alpha_s(\mu^2)}{2\pi}\right) \\
&\times \Bigg\{ \left(1+\cos^2\theta_1\right)\Bigg[-\left(1+x_1^2\right)\left(\frac{\ell n(1-x_1)}{1-x_1}\right)_+ - \frac{1+x_1^2}{(1-x_1)_+}\ell n\frac{\delta^2}{4} \\
&\qquad +\delta(1-x_1)\left(\frac{2\pi^2}{3}-\frac{9}{2}-\ell n^2\frac{\delta^2}{4}\right) - \frac{3}{2}\left(\frac{1}{1-x_1}\right)_+ - \frac{1}{2}\left(x_1-3\right)\Bigg] \\
&\quad + \left(1-3\cos^2\theta_1\right)\Bigg\} \\
&- \left[\frac{2}{s}\, F^{PC}(s)\right]\left[\alpha_{em}^2\, N_c \left(\frac{4\pi\mu^2}{(s/4)\sin^2\theta_1}\right)^{\epsilon} \frac{1}{\Gamma(1-\epsilon)}\, \frac{1}{x_1}\right] \\
&\quad \times \left(1+\cos^2\theta_1 - 2\epsilon\right) C_F \left(\frac{\alpha_s(\mu^2)}{2\pi}\right)\left[\left(\frac{4\pi\mu^2}{s}\right)^{\epsilon}\frac{1}{\Gamma(1-\epsilon)}\right] \\
&\quad \times \left\{\frac{1}{\epsilon^2} + \frac{1}{\epsilon}\left(\frac{3}{2} - \ell n\frac{\delta^2}{4}\right)\right\}\delta(1-x_1)\ . \qquad (102)
\end{aligned}
$$

As indicated in Eq. (94), $\hat{y}_{13}$ is always larger than zero for a fixed value of $x_1 \neq 1$. Therefore, $E_1 d\sigma^{(1)iso}_{e^+e^-\to qX}/d^3p_1$, defined in Eq. (102), is independent of $\mu^2_{\overline{\rm MS}}$. Furthermore, because there are no collinear subtraction terms for the isolated partonic cross section, the short-distance isolated partonic cross section $\hat{\sigma}^{(1)iso} = \sigma^{(1)iso}$ given in Eq. (102). We note that for $x_1 \neq 1$, Eq. (102) reduces to Eq. (84), as it should. However, as $x_1 \to 1$, the uncanceled $1/\epsilon^2$ and $1/\epsilon$ poles in Eq. (102) for $\hat{\sigma}^{(1)iso}$ signal a breakdown of conventional perturbative QCD factorization [5].

The singularities in Eq. (102) corresponding to the uncanceled poles are infrared in nature and, as expected, are proportional to $\delta(1-x_1)$. As explained above, the uncanceled poles come from the interval specified by the second term in Eq. (95). This interval results from the restricted phase space for soft real gluon emission due to the isolation constraints. These poles would be irrelevant if $x_1 \neq 1$. However, $x_1 \equiv x_\gamma/z$, and $x_1 = 1$ is kinematically allowed when $x_\gamma = 1/(1+\epsilon_h)$.

We conclude that the conventional factorization theorem for the cross section of isolated

photons in e^+e^- annihilation necessarily breaks down when $x_\gamma \sim 1/(1+\epsilon_h)$.

V. NUMERICAL RESULTS AND DISCUSSION

In this section, we present numerical results for the isolated photon cross section in hadronic final states of e^+e^- annihilation, and we discuss the consequences of the breakdown of conventional perturbative factorization.

In the analysis of Section IV, three regions are identified. In the first region, $x_\gamma < 1/(1+\epsilon_h)$, the isolated cross section is well behaved in perturbation theory except for an infrared logarithmic divergence as x_γ approaches $1/(1+\epsilon_h)$, associated uniquely with the $O(\alpha_s)$ quark-to-photon fragmentation component of the cross section. The second region is the singular point $x_\gamma = 1/(1+\epsilon_h)$. At this point, the isolated cross section is undefined in perturbation theory. It is the point at which the conventional factorization theorem breaks down. The third region is the region $x_\gamma > 1/(1+\epsilon_h)$. In this third region, but for the incompatibility of the collinear and cone definition of fragmentation, there should be no subtraction term and the isolated and inclusive cross sections would be identical. However, because of this incompatibility, the $O(\alpha_s)$ subtraction terms are finite in a very small interval $1/(1+\epsilon_h) < x_\gamma < x_\gamma^{\max}$, and the perturbative cross section is predicted to show a logarithmic divergence as x_γ approaches $1/(1+\epsilon_h)$ from above. This logarithmic divergence has a collinear origin. For $x_\gamma > x_\gamma^{\max}$ the isolated cross section equals the full inclusive cross section. All of these features are illustrated in the numerical results presented below.

The analytical expressions, Eqs. (80), (81) and (83), for the cross sections with x_γ less than $1/(1+\epsilon_h)$ should be useful for comparison with data from LEP. The expressions for $x_\gamma^{\max} > x_\gamma > 1/(1+\epsilon_h)$, Eqs. (86), (88) and (89) should not be taken seriously because of the logarithm, $\ell n((1+\epsilon_h) - 1/x_\gamma)$, caused by the incompatibility between the two definitions of the parton fragmentation. For $x_\gamma > x_\gamma^{\max}$, the isolated cross section equals to the inclusive cross section. Although the phase space above $x_\gamma = 1/(1+\epsilon_h)$ is small, the behavior of

the expressions for $x_\gamma > 1/(1+\epsilon_h)$ has important implications for the isolated photon cross section in hadronic collisions. In hadronic collisions, the influence of this limited phase space is enhanced after the hard cross section is convoluted with beam hadrons' parton distributions.

A. Numerical Results

Using the analytical results derived in the previous section, we evaluate the cross section for isolated photons at the LEP energy $\sqrt{s} \simeq M_Z$, and we compare this cross section with corresponding cross section for inclusive photons. In deriving our numerical results, we set $M_Z = 91.187$ GeV and $\Gamma_Z = 2.491$ GeV. The vector and axial-vector couplings and other constants are taken from Ref. [15]. The weak mixing angle $\sin^2\theta_w = 0.2319$. For the electromagnetic coupling strength α_{em}, we use the solution of the first order QED renormalization group equation, and let $\alpha_{em}(M_Z) = 1/128$ [1]. For the $O(\alpha_s)$ contributions, we employ a two-loop expression for $\alpha_s(\mu^2)$ with quark threshold effects handled properly. We set $\Lambda^{(4)}_{QCD} = 0.231$ GeV, which corresponds to $\alpha_s(M_Z) = 0.112$.

For the quark-to-photon and gluon-to-photon fragmentation functions, we use the analytical expressions provided in Ref. [16]. These fragmentation functions are leading-order functions. In principle, it would be more consistent to use $\overline{\rm MS}$ fragmentation functions evolved in next-to-leading order [1]. However, since our primary purpose here is to provide a theoretical framework for understanding the behavior of isolated photon production, not necessarily to present the most up-to-date numerical predictions, we believe these leading-order fragmentation functions are adequate for demonstrating the features of the cross section for isolated photons.

In presenting results, we divide our cross sections by an energy dependent cross section σ_0 that specifies the leading-order total hadronic event rate at each value of $\sqrt{s}$:

$$\sigma_0 = \frac{4\pi s}{3} \sum_q \left[\frac{2}{s} F_q^{PC}(s)\ \alpha_{em}^2(s) N_c \right]. \tag{103}$$

This procedure divides out overall multiplicative factors, and, in doing so, shows approximately what fraction of the total hadronic rate is represented by prompt photon production. One could, of course, divide instead by the next-to-leading-order total hadronic event rate, differing from Eq. (103) only by the overall factor $(1 + \alpha_s/\pi)$.

In Fig. 11, we compare the cross sections for isolated and inclusive photons as a function of the photon energy E_γ at $\sqrt{s}$ =91 GeV and $\theta_\gamma = 90°$. We set the renormalization scale equal to the fragmentation scale, and both of them equal to photon's energy. The isolation cone size is chosen to be $\delta = 20°$. The isolation energy parameters are chosen as $\epsilon_h = 0.05$ and $\epsilon_h = 0.15$ in Fig. 11(a) and Fig. 11(b), respectively. The value $\epsilon_h = 0.05$ is typical of LEP experiments, while $\epsilon_h = 0.15$ is used by CDF and D0 at the Fermilab Tevatron collider. As expected, the isolated cross section is finite and well-behaved in most of interval of E_γ less than the critical value $\sqrt{s}/2(1+\epsilon_h)$ (or $x_\gamma \ll 1/(1+\epsilon_h)$. The perturbatively calculated isolated cross section is less than the inclusive cross section in most of this interval, as it ought to be. When E_γ approaches $\sqrt{s}/2(1+\epsilon_h)$ (or $x_\gamma \to 1/(1+\epsilon_h)$), the perturbatively calculated isolated cross section becomes larger than inclusive cross section, which does not make physical sense, and it eventually approaches infinity when $x_\gamma = 1/(1+\epsilon_h)$, where conventional factorization breaks down. When E_γ approaches the critical value from above (i.e., $x_\gamma > 1/(1+\epsilon_h)$), the perturbatively calculated isolated cross section approaches negative infinity, a result of the term proportional to $\ell n((1+\epsilon_h) - 1/x_\gamma)$ in Eqs. (86), (88) and (89).

Figure 11(b) shows that the perturbatively calculated isolated cross section starts at negative infinity when $E_\gamma = \sqrt{s}/2(1+\epsilon_h)$. It increases as E_γ increases and quickly becomes equal to the inclusive cross section. Since the values of $x_\gamma^{\max}(\delta, \epsilon_h)$ in Eq. (50) and $x^{\max}(z, \delta, \epsilon_h)$ in Eq. (62) are very close to the critical value $1/(1+\epsilon_h)$, the region in which Eqs. (86), (88) and (89) are applicable is extremely small. Therefore, the isolated cross section is equal to the inclusive cross section in most of the interval of E_γ larger than the critical value $\sqrt{s}/2(1+\epsilon_h)$ (or $x_\gamma > 1/(1+\epsilon_h)$).

In Fig. 12, we show the breakdown of the isolated cross section in terms of contributions from individual pieces. The isolated cross section is plotted as a function of E_γ at

$\sqrt{s} = 91$ GeV and scattering angle $\theta_\gamma = 90°$. We choose $\delta = 20°$, $\epsilon_h = 0.15$ and $\epsilon_h = 0.30$ in Fig. 12(a) and Fig. 12(b), respectively. We use the label "0th-Frag" for the lowest-order fragmentation contribution, "Direct" for $O(\alpha_{em})$ direct production, and "q-Frag" and "g-Frag" for the $O(\alpha_s)$ quark and gluon fragmentation contributions, respectively. The curves in Fig. 12 show that the breakdown of factorization is associated with the $O(\alpha_s)$ quark fragmentation contribution, which is infrared in nature. All one-loop contributions approach negative infinity as E_γ approaches the critical value from above, confirming that this divergence is of collinear origin, caused by the incompatibility between the two definitions of parton fragmentation: exact collinear long-distance fragmentation and the short-distance contribution with a finite cone size.

In Fig. 13, we examine the predicted θ_γ dependence of the isolated cross section when E_γ is about half of the critical value. We plot the isolated cross section as a function of scattering angle θ_γ for $E_\gamma = 20$ GeV. Other parameters are chosen as shown in the figure. There is no contribution from the leading order quark fragmentation, and the $O(\alpha_s)$ contributions are negligible at this energy. The angular dependence of the isolated cross section at $\sqrt{s} \simeq 20$ GeV is determined by the direct contribution, which has both $1+\cos^2\theta_\gamma$ and $\sin^2\theta_\gamma$ contributions (c.f., Eq. (80)).

In Figs. 11–13, we set the renormalization and fragmentation scale to be $\mu = E_\gamma$. Dependence of the isolated cross section on μ is examined in Fig. 14. We plot the isolated cross section as a function of μ/E_γ at $\sqrt{s} = 91$ GeV, $\theta_\gamma = 90°$, and a fixed $E_\gamma = 20$ GeV. Other parameters are as shown in the figure. As expected, the isolated cross section has a very small scale dependence. Isolation eliminates most of the fragmentation contributions, and the dominant direct contribution, Eq. (80), is not affected by strong interactions. It has neither renormalization nor fragmentation scale dependence.

Dependence on ϵ_h is strong in the region near $x_\gamma \sim 1/(1+\epsilon_h)$, but the perturbative calculation is not reliable in this region. In Fig. 15, we plot the isolated cross section as a function of ϵ_h at a fixed value of $E_\gamma = 20$ GeV, about half of the critical value. Relatively small dependence on ϵ_h is observed. As expected, Fig. 15 shows that the isolated cross

section grows as ϵ_h increases. At larger ϵ_h, more hadronic energy is allowed in the isolation cone, and consequently, more events contribute to the isolated cross section.

The isolated cross section is predicted to show a specific $\ell n\, \delta^2$ dependence on the cone size δ. This prediction is valid for small values of δ since we neglect throughout terms proportional to finite powers of δ. In doing our analysis, we explicitly constrain $\delta \neq 0$. If δ is set to zero before the phase space integrals are done (e.g., in Eqs. (53), (69), and (95)) then we would find $\hat{\sigma}^{(1)sub} = 0$ and $\hat{\sigma}^{isol} = \hat{\sigma}^{incl}$. For $x_\gamma < 1/(1+\epsilon_h)$, the $\ell n\, \delta^2$ dependence of the isolated cross section is displayed explicitly in Eqs. (80), (82), and (84).

B. Discussion

According to the conventional factorization theorem of perturbative QCD [10], the one-loop fragmentation contributions derived here become the collinear counter-terms for the two-loop direct contribution to $e^+e^- \to \gamma X$ at order $O(\alpha_{em}\alpha_s)$. In similar fashion to the derivation of Eq. (21), we apply Eq. (9) perturbatively to the order $\alpha_{em}\alpha_s$. We obtain

$$\begin{aligned}
\sigma^{(2)sub}_{e^+e^-\to\gamma X}\Big|_{E_q(or\, E_{\bar{q}})\geq\epsilon_h E_\gamma} &= \hat{\sigma}^{(2)sub}_{e^+e^-\to\gamma X}(x_\gamma)\dot{\otimes}D^{(0)}_{\gamma\to\gamma}(z) + \hat{\sigma}^{(2)incl}_{e^+e^-\to\gamma X}(x_\gamma)\ddot{\otimes}D^{(0)}_{\gamma\to\gamma}(z) \\
&+ \hat{\sigma}^{(1)sub}_{e^+e^-\to qX}(x_q)\dot{\otimes}D^{(1)}_{q\to\gamma}(z) + \hat{\sigma}^{(1)incl}_{e^+e^-\to qX}(x_q)\ddot{\otimes}D^{(1)}_{q\to\gamma}(z) \\
&+ \hat{\sigma}^{(0)sub}_{e^+e^-\to qX}(x_q)\dot{\otimes}D^{(2)}_{q\to\gamma}(z) + \hat{\sigma}^{(0)incl}_{e^+e^-\to qX}(x_q)\ddot{\otimes}D^{(2)}_{q\to\gamma}(z) \\
&+ (q\to\bar{q})\ . \qquad (104)
\end{aligned}$$

Since the zeroth-order subtraction term $\hat{\sigma}^{(0)sub}_{e^+e^-\to qX}$ vanishes, and the zeroth order photon-to-photon fragmentation function $D^{(0)}_{\gamma\to\gamma}(z) = \delta(1-z)$, the factorized expression for the two-loop short-distance hard-part becomes

$$\begin{aligned}
\hat{\sigma}^{(2)sub}_{e^+e^-\to\gamma X}(x_\gamma) &= \sigma^{(2)sub}_{e^+e^-\to\gamma X}\Big|_{E_q(or\, E_{\bar{q}})\geq\epsilon_h E_\gamma} \\
&- \hat{\sigma}^{(1)sub}_{e^+e^-\to qX}(x_q)\dot{\otimes}D^{(1)}_{q\to\gamma}(z) - \hat{\sigma}^{(1)incl}_{e^+e^-\to qX}(x_q)\ddot{\otimes}D^{(1)}_{q\to\gamma}(z) \\
&- \hat{\sigma}^{(0)incl}_{e^+e^-\to qX}(x_q)\ddot{\otimes}D^{(2)}_{q\to\gamma}(z) - (q\to\bar{q})\ . \qquad (105)
\end{aligned}$$

It is clear from Eq. (105) that the one-loop subtraction term, $\hat{\sigma}^{(1)sub}_{e^+e^-\to qX}$ derived in this paper, Eqs. (71) and (73), becomes a collinear counter-term for the two-loop direct contribution.

Therefore, due to the breakdown of factorization at $x_\gamma = 1/(1+\epsilon_h)$ at one-loop order and the fact that the perturbatively calculated isolated cross section is larger than the corresponding inclusive cross section, the higher-order contributions to the isolated cross sections may be ill-defined as well. To resolve this issue, it will be important and necessary to investigate possible alternative definitions of the cross section of isolated photons to all orders in perturbation theory.

In Eq. (2), we define the isolated cross section as a difference between the inclusive cross section and a subtraction term. The inclusive cross section is well-defined in perturbative QCD [1]. Since the isolated cross section is an experimental measurable and known to be finite, the subtraction term, defined in Eq. (2), should be finite as well. It is not difficult to show, as we have in this paper, that the subtraction term is an infrared sensitive quantity in perturbation theory. Therefore, the issue is whether we can find a scheme to consistently factorize the infrared sensitive quantity into a perturbatively calculable infrared safe hard-part convoluted with a well-defined long-distance universal function, such as the fragmentation function.

Although the breakdown of factorization is demonstrated in this paper only at one-loop level in perturbation theory, the following intuitive argument generalizes our thinking. As remarked in Sec. II, the subtraction term can be viewed as a "cross section" for a photon "jet" with photon momentum ℓ and hadronic energy E_h^{cone} in the "jet" cone, with the hadronic energy required to be larger than $E_{\rm max} = \epsilon_h E_\gamma$. This "jet cross section" is an integrated jet cross section, where "integrated" denotes the cross section for "jet" events with hadronic energy greater than a fixed minimum value ($E_{\rm max} = \epsilon_h E_\gamma$) and up to a whatever maximum value is allowed by the kinematics. Experience with the definition and calculation of jet cross section [14,17] suggests that the integrated "jet cross section" could be finite in perturbative QCD, as long as we do not specify details within the jet. However, if we insist on determining the energy of one specific parton within the "jet", and ask how this parton fragments into the observed photon, we will most likely encounter an incomplete cancellation of infrared and collinear singularities. Introduction of parton-to-photon fragmentation functions for the

cross section of isolated photons is similar to asking for the details within the photon "jet". Further analysis of these issues is beyond the scope of the present paper.

C. Phenomenology

The $O(\alpha_{em})$ direct contribution to the isolated cross section is dominant over most of the region $x_\gamma < 1/(1+\epsilon_h)$ where perturbation theory is reliable. This statement is illustrated in Figs. 12-15. Correspondingly, a direct comparison of our expressions with data on isolated prompt photon production is tantamount primarily to a verification of the $O(\alpha_{em})$ expression presented in Eq. (80). In this expression, we display the explicit dependence of the cross section on E_γ, θ_γ, and δ. On the other hand, an important goal of investigations of $e^+e^- \to \gamma X$ is also the extraction of quark-to-photon and gluon-to-photon fragmentation functions [11–13]. Our analysis of this paper indicates that the task is not straightforward. Not only is the direct contribution dominant over a large interval if ϵ_h is small, but as we demonstrated to order $O(\alpha_s)$, the perturbatively computed quark-to-parton fragmentation contribution to the isolated cross section is infrared singular in the neighborhood of $x_\gamma = 1/(1+\epsilon_h)$. This means that we cannot offer a reliable theoretical expression for comparison with experiment in this region. We expect that further theoretical work in the near future will lead to a resolution of this unsatisfactory situation. Meanwhile, we suggest a possible procedure for analysis of the data. We suggest that the $O(\alpha_{em})$ direct contribution, specified in Eq. (80), be subtracted from the data. Since the direct contribution is of purely electromagnetic origin at $O(\alpha_{em})$, it is not subject to hadronic uncertainties. After the subtraction is done, one is left with a sample of events that may be attributed to $O(\alpha_s)$ quark-to-photon and gluon-to-photon fragmentation. It would be instructive to examine the E_γ, θ_γ, and δ dependence of this subtracted sample.

Isolation enhances the $O(\alpha_{em})$ direct contribution and eliminates the leading-order quark-to-photon fragmentation contribution for x_γ less than the critical value $1/(1+\epsilon_h)$. It has been suggested [2] that the region in which the contribution from leading-order quark-to-

photon fragmentation is important can be enlarged if ϵ_h is chosen to be relatively large. In Figs. 12(b) and 12(c), the dashed curve shows the contribution from the leading-order fragmentation contribution; it contributes only in the region above $x_\gamma = 1/(1+\epsilon_h)$. The leading-order fragmentation contribution dominates in this region, and the isolated cross section is essentially the same as the inclusive cross section [1]. Experimental measurement of prompt photons in this region is difficult both because the rate is low and because clean identification of a *prompt* photon signal is problematic if ϵ_h is relatively large. When ϵ_h is large, the hadronic energy in the cone makes it difficult on an event-by-event basis to be certain the photon does not result from π^o or η decay, or from other hadronic processes.

We turn next to implications of our analysis for the computation of isolated prompt photon cross sections at hadron colliders. In hadron reactions, the lowest-order subprocesses are the two $O(\alpha_s\alpha_{em})$ direct subprocesses, $q + g \to q + \gamma$ and $q + \bar{q} \to g + \gamma$, along with the lowest-order fragmentation subprocesses. In the lowest-order fragmentation, various $O(\alpha_s^2)$ two-parton to two-parton subprocesses are followed by leading-order long distance quark-to-photon or gluon-to-photon fragmentation. In computing prompt photon production to next-to-leading order in QCD, one must compute all $O(\alpha_s^2\alpha_{em})$ direct subprocesses and include fragmentation at next-to-leading order. It is at this level that problems of the type we find in our study of electron-positron annihilation will also be encountered in the hadronic case. Specifically, the next-to-leading order quark fragmentation contribution is ill defined owing to the infrared problem identified in our analysis. In their treatment of prompt photon production, Baer, Ohnemus, and Owens [7] include the direct contributions through $O(\alpha_s^2\alpha_{em})$, but they include fragmentation through lowest-order only. Their results are therefore not affected by the infrared problem. The studies of Gordon, Vogelsang, and collaborators [9] include fragmentation through next-to-leading order.

It is not our intent in this paper to provide a new analysis of the hadronic case. Rather, we wish to point out that the infrared sensitivity of the next-to-leading order quark-to-photon fragmentation contribution is enhanced in the hadronic case. We also suggest a temporary phenomenological remedy. In hadron-hadron collisions, we are interested in the

production of prompt photons as a function of the photon's transverse momentum, p_T. Invoking factorization, and continuing to use ℓ to denote the four-vector momentum of the photon, we write the inclusive or the isolated cross section in $hadron(A)+hadron(B) \to \gamma X$ as

$$E_\gamma \frac{d\sigma_{AB\to\gamma X}}{d^3\ell} = \sum_{a,b} \int dx_a\, \phi_{a/A}(x_a)\, dx_b\, \phi_{b/B}(x_b)\, E_\gamma \frac{d\sigma_{ab\to\gamma X}}{d^3\ell} \ . \tag{106}$$

The sum is taken over all initial partons $(q, \bar{q}, g)$ in the incident hadrons, and $\phi(x)$ are parton density distributions. The partonic level cross section is expressed as

$$E_\gamma \frac{d\sigma_{ab\to\gamma X}}{d^3\ell} = \sum_{c} \int \frac{dz}{z}\, E_c \frac{d\hat{\sigma}_{ab\to cX}}{d^3 p_c} \left(p_c = \frac{\ell}{z} \right) \frac{D_{c\to\gamma}(z)}{z} \ , \tag{107}$$

where $c = \gamma, q, \bar{q}$, or g. If the factorization theorem holds for isolated photons, the partonic hard-parts $\hat{\sigma}_{ab\to cX}$ in Eq. (107) should be finite for isolated photons and should be smaller than the corresponding hard parts for the inclusive cross section. This is not the case for the perturbatively computed quark fragmentation contribution at one-loop, as we now illustrate.

To streamline the discussion we begin by defining a parton-parton flux $\Phi(\tau)$,

$$\Phi_{ab}(\tau) = \int_\tau^1 \frac{dx}{x}\, \phi_{a/A}(x)\, \phi_{b/B}(\tau/x) \ , \tag{108}$$

where $\tau \equiv x_a\, x_b$. To exploit our electron-positron results most conveniently, we limit our discussion to the contribution in Eq.(106) associated with the quark-antiquark initial state, and, further, we take only the term in which the flavors of the initial and final quarks differ: $q' + \bar{q}' \to q + \bar{q} + g$, where q fragments to γ. We point out, however, that there is a next-to-leading order quark fragmentation contribution associated with almost all subprocesses. Our illustration is therefore much more general than the specific example we treat. We further specialize to prompt photon production at zero rapidity (i.e., at 90° in the hadron-hadron center-of-mass frame), and ignore real gluon emission from the initial-state quark (q') antiquark ($\bar{q}'$) and from the s-channel virtual gluon (g). As an expedient approximation we take equal values for the partonic fractions, $x_a = x_b = x = \sqrt{\tau}$. This latter approximation allows us, in the isolated case, to use our Eqs. (83) and (84) directly, setting $\theta_\gamma = 90°$ in

Eq. (84). Likewise, in the inclusive case, we use our Eqs. (78) and (79) directly, setting $\theta_\gamma = 90^\circ$ in Eq. (79). The normalization factor differs, of course, in the hadron case. In Eqs. (79) and (84), we replace

$$s \to \hat{s} = x_a\, x_b\, s = \tau\, s \ ; \tag{109a}$$

$$\frac{2}{s} F_q^{PC}(s) \to \frac{1}{\hat{s}^2} \ ; \tag{109b}$$

$$\alpha_{em}^2 \to \alpha_s^2 \ ; \tag{109c}$$

$$N_c\, C_F \to \frac{N^2-1}{N^3} \ . \tag{109d}$$

In the translation to the hadronic case, the variable x_γ becomes $\hat{x}_T$ where $\hat{x}_T = 2p_T/\sqrt{\hat{s}} \sim x_T/x$ with $x_T = 2p_T/\sqrt{s}$.

The special one-loop quark fragmentation contribution to the observed cross section takes the form

$$E_\gamma \frac{d\sigma_{AB\to\gamma X}}{d^3\ell} \sim \int_{x_T^2}^1 d\tau\ \Phi_{q'\bar{q}'}(\tau)\ E_\gamma \frac{d\sigma_{q'\bar{q}'\to\gamma X}}{d^3\ell}(\tau) \quad + \quad \text{other subprocesses} \ . \tag{110}$$

In Eq. (110), the one-loop contribution $E_\gamma d\sigma_{q'\bar{q}'\to\gamma X}/d^3\ell(\tau)$ to inclusive [or isolated] cross section is obtained from Eq. (79) [or Eq. (84)] with the replacements defined in Eq. (109).

In Fig. 16, we present the one-loop quark-to-photon fragmentation contributions to the inclusive and isolated prompt photon cross sections as a function of the scaling variable x_γ in e^+e^- annihilation. The region of infrared instability in the neighborhood of $x_\gamma = 1/(1+\epsilon_h)$ is evident, as is the fact that the isolated cross section exceeds the inclusive in part of the x_γ interval.

In Fig. 17, we show the integrand in Eq. (110) obtained after convoluting the parton flux of Eq. (108) with the one-loop contributions in Fig. 16 (with the replacements in Eq. (109)). In obtaining Fig. 17, we use CTEQ3M parton distributions [18] to compute the effective parton flux, $\Phi_{q'\bar{q}'}(\tau)$ with $q' = u$ (up quark); the final-state quark flavor is chosen as $q = d$ (down quark). The features demonstrated in Fig. 17 are independent of the choice of quark flavors.

The one-loop fragmentation contribution to the hadronic cross section at a given value of transverse momentum p_T is obtained by computing the area under the curve in Fig. 17 from $x_T = 2p_T/\sqrt{s}$ to 1. It is evident that the convolution with the parton flux substantially enhances the influence of the region of infrared sensitivity. The divergences above and below the point $\hat{x}_T = x_T/\sqrt{\tau} = 1/(1+\epsilon_h)$ [or $x = \sqrt{\tau} = x_T(1+\epsilon_h)$] are integrable logarithmic divergences, and thus they yield a finite contribution if an integral is done over all x (or all τ). However, we stress that the perturbatively calculated one-loop partonic cross section $E_q\, d\hat{\sigma}^{iso}_{q'\bar{q}'\to qX}$, obtained from Eq. (84), has an inverse-power divergence as $x_q \to 1$ and has uncanceled $1/\epsilon$ poles in dimensional regularization [5]. The divergence for $x_\gamma < 1/(1+\epsilon_h)$ becomes a logarithmic divergence only after convolution with a long-distance fragmentation function. The theory is not defined at the point $\hat{x}_T = 1/(1+\epsilon_h)$, and it would be inappropriate to take the perturbatively calculated cross section at face value when it exceeds the inclusive cross section.

As remarked earlier, a new theoretical definition of the isolated photon cross section is desirable, along the lines of a "photon jet" definition. It would be infrared safe to all orders in α_s. Presumably, the new definition would avoid parton-to-photon fragmentation functions. Meanwhile, we propose a simple phenomenological remedy to deal with infrared problem illustrated in Figs. 16 and 17. In calculations of isolated prompt photon cross sections in hadron-hadron reactions, we suggest that the perturbatively calculated one-loop quark-to-photon fragmentation contribution to the isolated cross section be used only in the region of phase space in which it is calculated to be smaller than the inclusive rate. Elsewhere, the one-loop inclusive contribution should be used as an *upper bound*.

ACKNOWLEDGEMENTS

We thank George Sterman for helpful discussions. X. Guo and J. Qiu are grateful for the hospitality of Argonne National Laboratory where a part of this work was completed. Work in the High Energy Physics Division at Argonne National Laboratory is supported by the

U.S. Department of Energy, Division of High Energy Physics, Contract W-31-109-ENG-38. The work at Iowa State University is supported in part by the U.S. Department of Energy under Grant Nos. DE-FG02-87ER40731 and DE-FG02-92ER40730.

REFERENCES

[1] E. L. Berger, X. Guo, and J.-W. Qiu, Phys. Rev. **D53**, 1124 (1996), and references therein.

[2] E. W. N. Glover and W. J. Stirling, Phys. Lett. **B295**, 128 (1992); E. W. N. Glover and A. G. Morgan, Phys. Lett. **B324**, 487 (1994).

[3] Z. Kunszt and Z. Trocsanyi, Nucl. Phys. **B394**, 139 (1993).

[4] E. L. Berger, X. Guo, and J.-W. Qiu, in DPF '92, Proceedings of the 7th Meeting of the APS Division of Particles and Fields, Fermilab, November, 1992; ed. by C. H. Albright *et al.* (World Scientific, Singapore, 1993), Vol. 2, pp. 957-960.

[5] E. L. Berger, X. Guo, and J.-W. Qiu, Phys. Rev. Lett. **76**, 2234 (1996).

[6] E. L. Berger and J.-W. Qiu, Phys. Lett. **B248**, 371 (1990); E. L. Berger and J.-W. Qiu, Phys. Rev. **D44**, 2002 (1991).

[7] H. Baer, J. Ohnemus, and J. F. Owens, Phys. Rev. **D42**, 61 (1990).

[8] P. Aurenche *et al*, Nucl. Phys. **B399**, 34 (1993).

[9] L. E. Gordon and W. Vogelsang, Phys. Rev. **D48**, 3136 (1993) and **D50**, 1901 (1994); M. Glück, L. E. Gordon, E. Reya, and W. Vogelsang, Phys. Rev. Lett. **73**, 388 (1994).

[10] G. Altarelli, R. K. Ellis, G. Martinelli, and S. Y. Pi, Nucl. Phys. **B160**, 301 (1979); W. Furmanski and R. Petronzio, Phys. Lett. **B97**, 437 (1980); G. Gurci, W. Furmanski, and R. Petronzio, Nucl. Phys. **B175**, 27 (1980); J.C. Collins, D.E. Soper and G. Sterman, in *Perturbative Quantum Chromodynamics*, edited by A.H. Mueller (World Scientific, Singapore, 1989).

[11] P. D. Acton *et al.*, OPAL Collaboration, Z. Phys. **C58**, 405 (1993); D. Buskulic *et al.*, ALEPH Collaboration, Z. Phys. **C57**, 17 (1993); P. Abreu *et al.*, DELPHI Collaboration, Z. Phys. **C53**, 555 (1992); O. Adriani *et al.*, L3 Collaboration, Phys. Lett. **B292**,

472 (1992).

[12] D. Buskulic *et al.*, ALEPH Collaboration, Z. Phys. **C69**, 365 (1996).

[13] P. Mättig, H. Spiesberger, and W. Zeuner, Z. Phys. **C60**, 613 (1993).

[14] G. Sterman and S. Weinberg, Phys. Rev. Lett. **39**, 1436 (1977).

[15] Particle Data Group, Phys. Rev. **D50**, 1173 (1994).

[16] J.F. Owens, Rev. Mod. Phys. **59**, 465 (1987).

[17] S. Ellis, Z. Kunszt, and, D. Soper, Phys. Rev. Lett. **64**, 2121 (1990) and Phys. Rev. **D46**, 192 (1992); S. D. Ellis and D. Soper, Phys. Rev. **D48**, 3160 (1993).

[18] H.L. Lai *et al.*, CTEQ Collaboration, Phys. Rev. **D51**, 4763 (1995).

FIGURES

FIG. 1. Illustration of an isolation cone about the direction of the photon's momentum.

FIG. 2. Illustration of $e^+e^- \to \gamma X$ in an m parton state: $e^+e^- \to cX$ followed by fragmentation $c \to \gamma X$.

FIG. 3. Illustration of an isolation cone containing a parton c that fragments into a γ plus hadronic energy E_{frag}. In addition, the cone includes a gluon that fragments giving hadronic energy E_{parton}.

FIG. 4. Lowest order, $O\left(\alpha_{em}^o \alpha_s^o\right)$, photon production through quark fragmentation.

FIG. 5. Feynman diagrams for $e^+e^- \to \gamma q\bar{q}$.

FIG. 6. Order α_s Feynman diagram for the parton level fragmentation function $D_{q\to\gamma}^{(1)}(z)$.

FIG. 7. Order α_s Feynman diagrams for $e^+e^- \to q\bar{q}g$ that contribute to $e^+e^- \to \gamma X$ via $g \to \gamma$ fragmentation.

FIG. 8. Contributions to the $O(\alpha_s)$ cross section $\sigma_{e^+e^-\to qX}^{(1)}$; both real gluon emission diagrams ($e^+e^- \to q\bar{q}g$) and virtual gluon exchange terms are drawn.

FIG. 9. Order α_s Feynman diagrams for the parton level fragmentation function $D_{q\to q}^{(1)}(z)$.

FIG. 10. Center of mass coordinate axes of an e^+e^- collision with the z-axis being the direction of the observed photon.

FIG. 11. Comparison of the normalized cross sections for isolated and inclusive photons in $e^+e^- \to \gamma X$ as a function of photon energy E_γ: (a) $\epsilon_h = 0.05$; (b) $\epsilon_h = 0.15$.

FIG. 12. Normalized isolated photon cross section as a function of photon energy E_γ: (a) $\epsilon_h = 0.15$; (b) $\epsilon_h = 0.30$. The solid line is a the sum of contributions from all individual subprocesses. Shown also are the individual contributions from the separate subprocesses. The $O(\alpha_{em})$ direct contribution (upper dotted line) nearly saturates the total contribution for $x_\gamma < 1/(1+\epsilon_h)$. The dashed line for $x \geq 1/(1+\epsilon_h)$ shows the $O(\alpha_{em}^0 \alpha_s^0)$ fragmentation contribution. The $O(\alpha_s)$ quark-to-photon and gluon-to-photon fragmentation contributions are illustrated with the dot-dashed and the lower dotted lines, respectively.

FIG. 13. Normalized isolated photon cross section at $E_\gamma = 20$ GeV as a function of θ_γ. The solid line is the sum of all contributions. The $O(\alpha_{em})$ direct contribution (dashed line) essentially saturates the total. The $O(\alpha_s)$ quark-to-photon (dot-dashed) and gluon-to-photon (dotted) contributions are also shown.

FIG. 14. Normalized isolated photon cross section as a function of μ/E_γ. There is no leading order fragmentation contribution: "0-Frag" at $E_\gamma = 20$ GeV. The labeling of the curves is the same as in Fig. 13.

FIG. 15. Normalized isolated photon cross section as a function of ϵ_h. There is no leading order fragmentation contribution: "0-Frag" at $E_\gamma = 20$ GeV. The labeling of the curves is the same as in Fig. 13.

FIG. 16. Comparison of the one-loop quark fragmentation contributions to the isolated cross section and the inclusive cross section in $e^+e^- \to \gamma X$ as a function of $x_\gamma = 2E_\gamma/\sqrt{s}$.

FIG. 17. Integrand of Eq. (110) as a function of $x_T/\sqrt{\tau} = x_T/x$ for $p\bar{p} \to \gamma X$ at $\sqrt{s} = 1.8$ TeV and $p_T^\gamma = 20$ GeV and rapidity zero. The isolation parameters are $\epsilon_h = 0.15$ and $\delta = 20^\circ$.

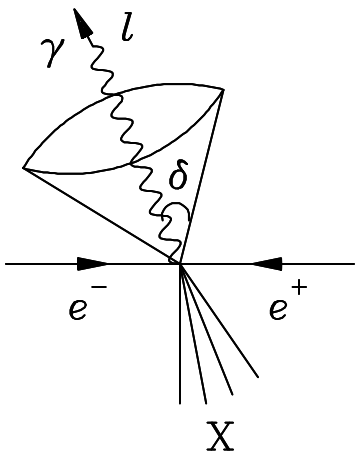

Fig.1

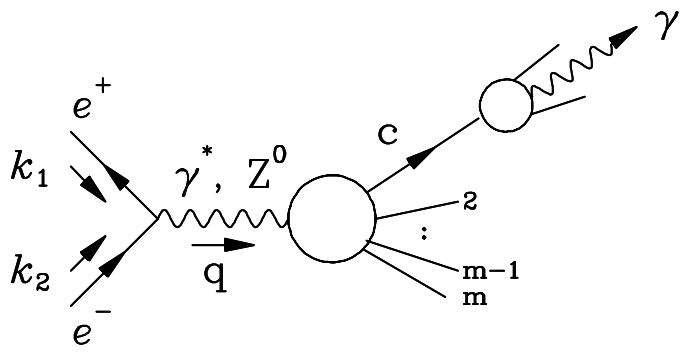

Fig.2

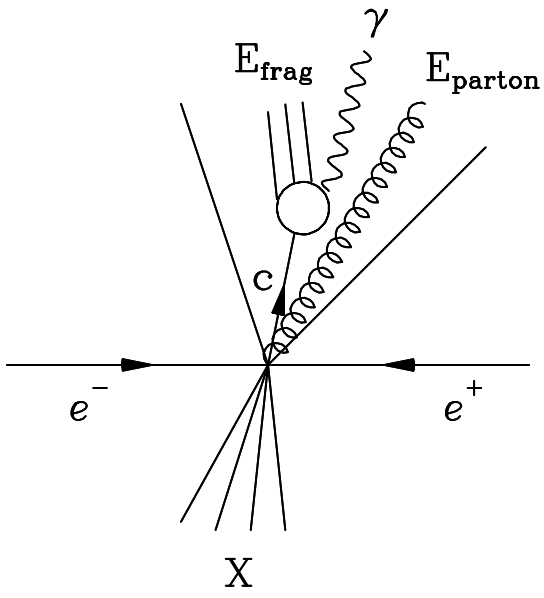

Fig.3

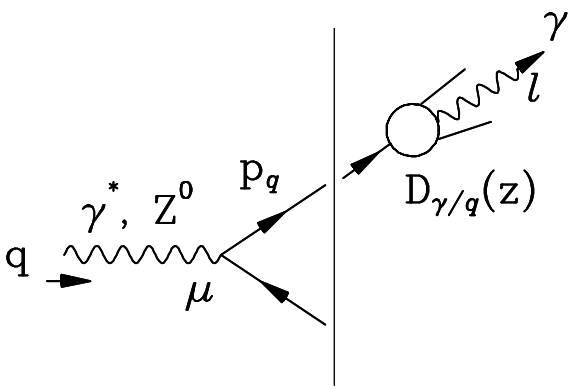

Fig.4

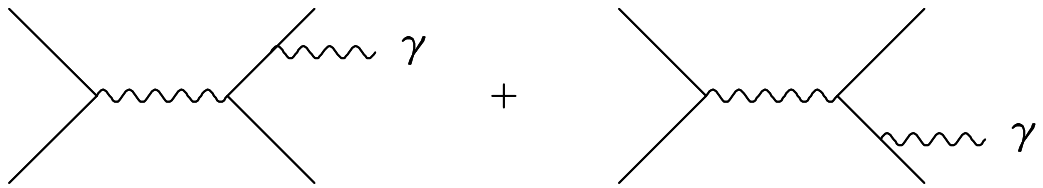

Fig.5

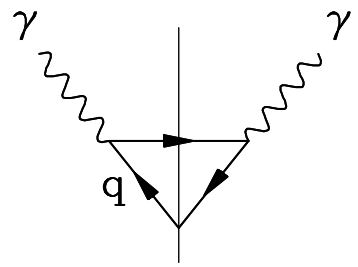

Fig.6

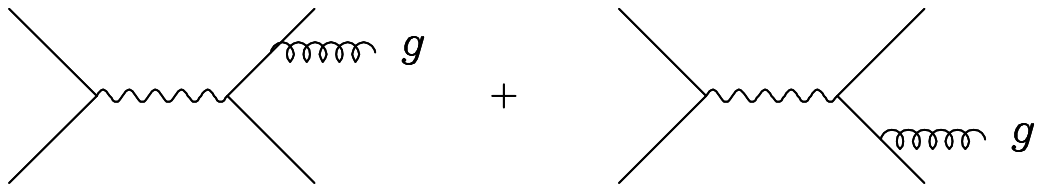

Fig.7

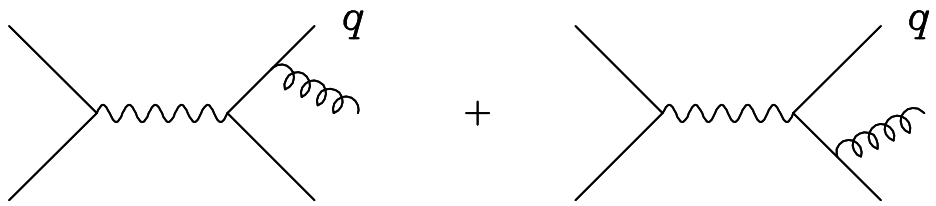

(a)

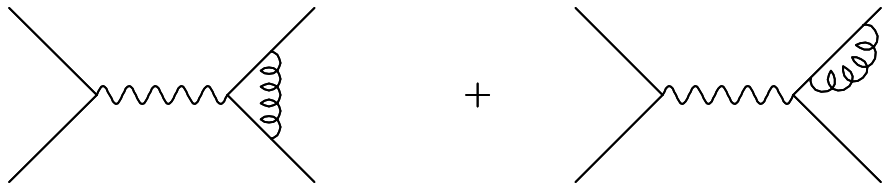

(b)

Fig.8

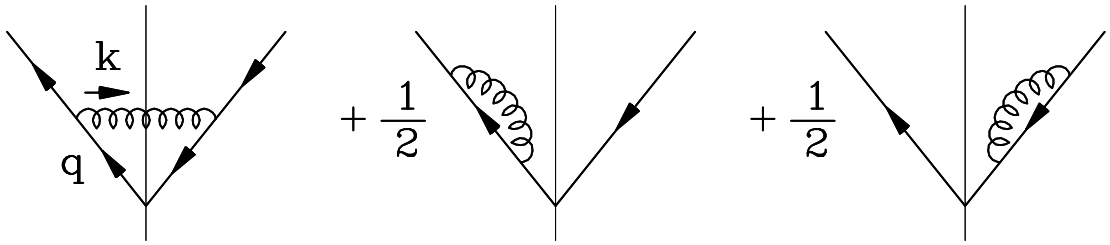

Fig.9

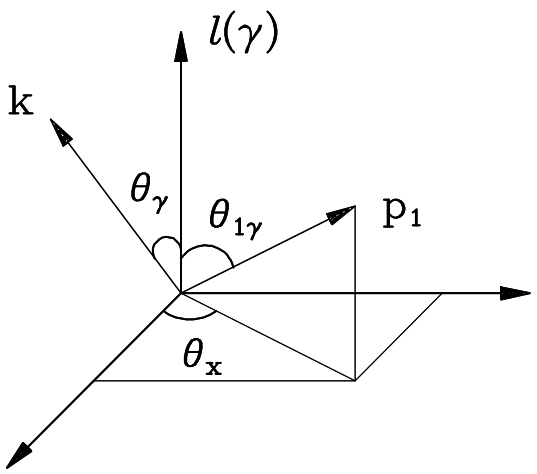

Fig.10

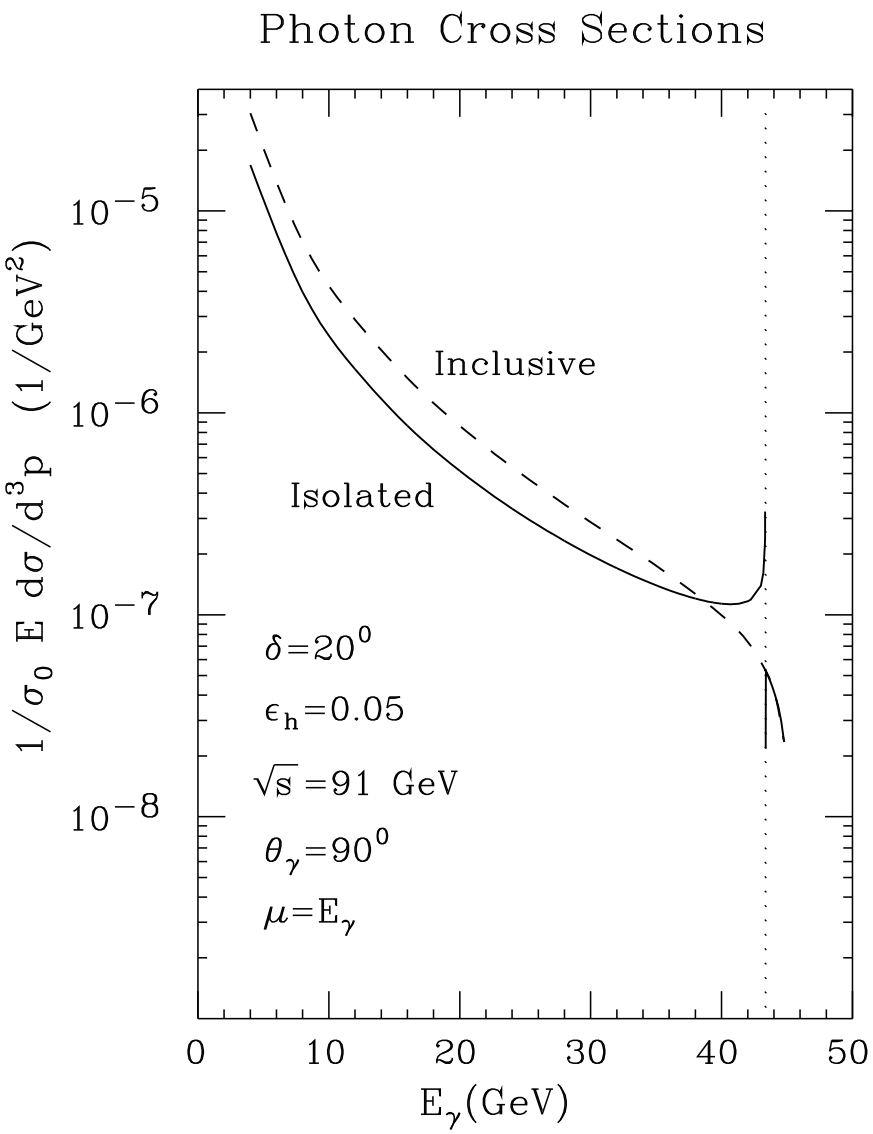
Photon Cross Sections
$1/\sigma_0\ E\ d\sigma/d^3p\ \ (1/GeV^2)$
10^{-5}
10^{-6}
10^{-7}
10^{-8}
Inclusive
Isolated
$\delta=20^0$
$\epsilon_h=0.05$
$\sqrt{s}=91$ GeV
$\theta_\gamma=90^0$
$\mu=E_\gamma$
0
10
20
30
40
50
E_γ(GeV)

Fig.11−(a)

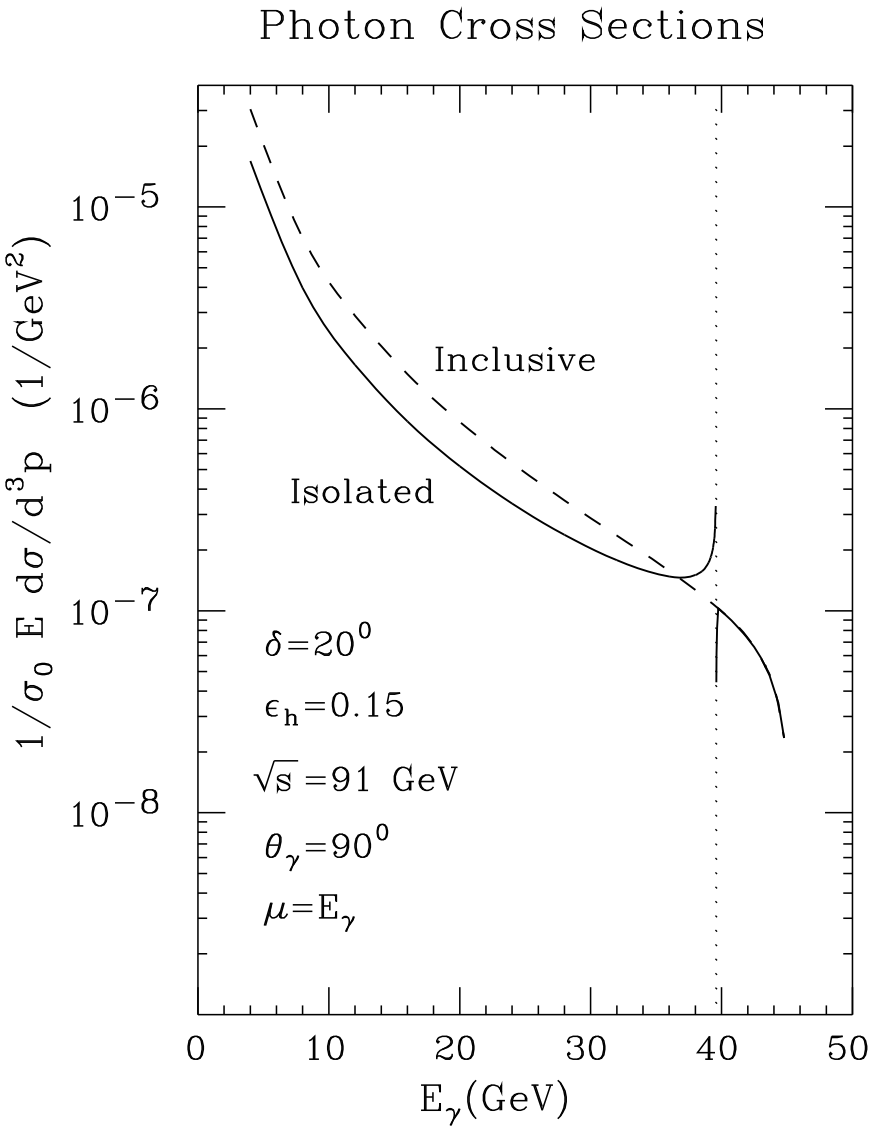
Photon Cross Sections
$1/\sigma_0\ E\ d\sigma/d^3p\ \ (1/GeV^2)$
10^{-5}
10^{-6}
10^{-7}
10^{-8}
Inclusive
Isolated
$\delta=20^0$
$\epsilon_h=0.15$
$\sqrt{s}=91$ GeV
$\theta_\gamma=90^0$
$\mu=E_\gamma$
0
10
20
30
40
50
E_γ(GeV)

Fig.11−(b)

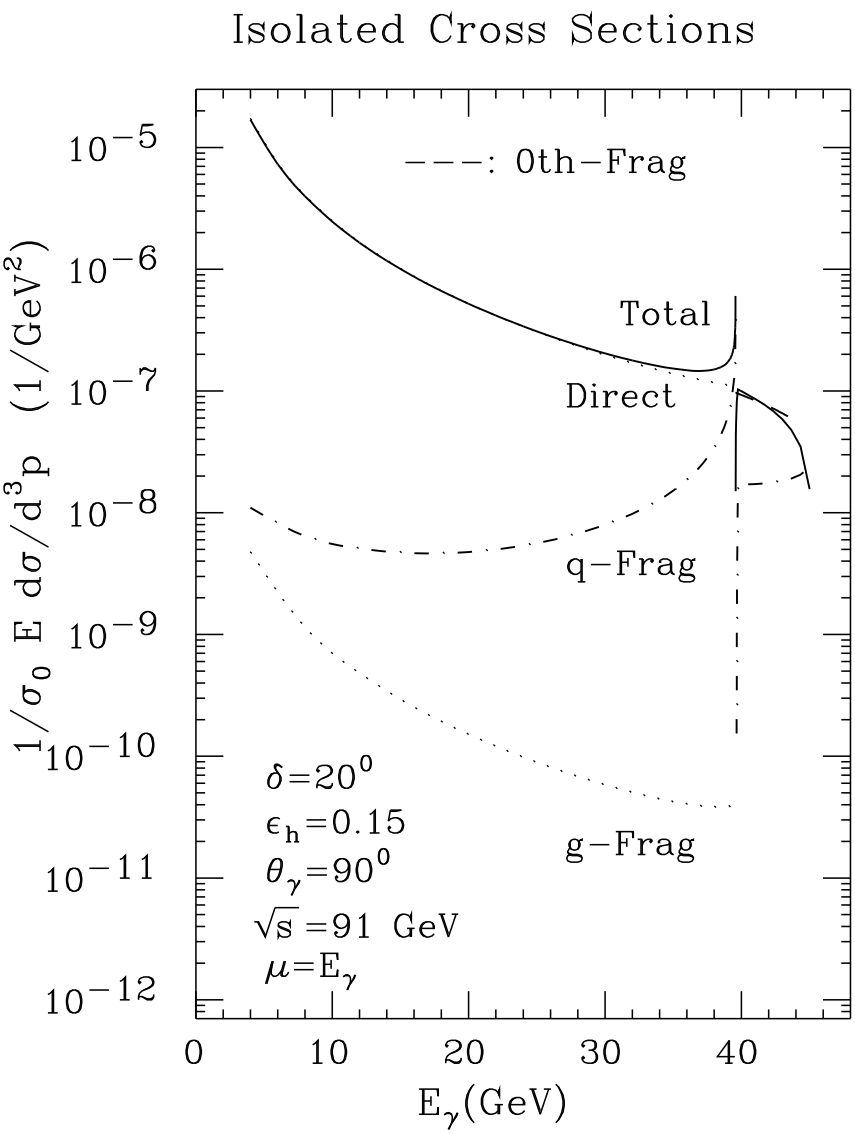
Isolated Cross Sections
---: 0th-Frag
Total
Direct
q-Frag
g-Frag
$\delta=20^0$
$\epsilon_h=0.15$
$\theta_\gamma=90^0$
$\sqrt{s}=91$ GeV
$\mu=E_\gamma$
$1/\sigma_0\ E\ d\sigma/d^3p\ \ (1/GeV^2)$
$E_\gamma(GeV)$
10^{-5}
10^{-6}
10^{-7}
10^{-8}
10^{-9}
10^{-10}
10^{-11}
10^{-12}
0
10
20
30
40

Fig.12-(a)

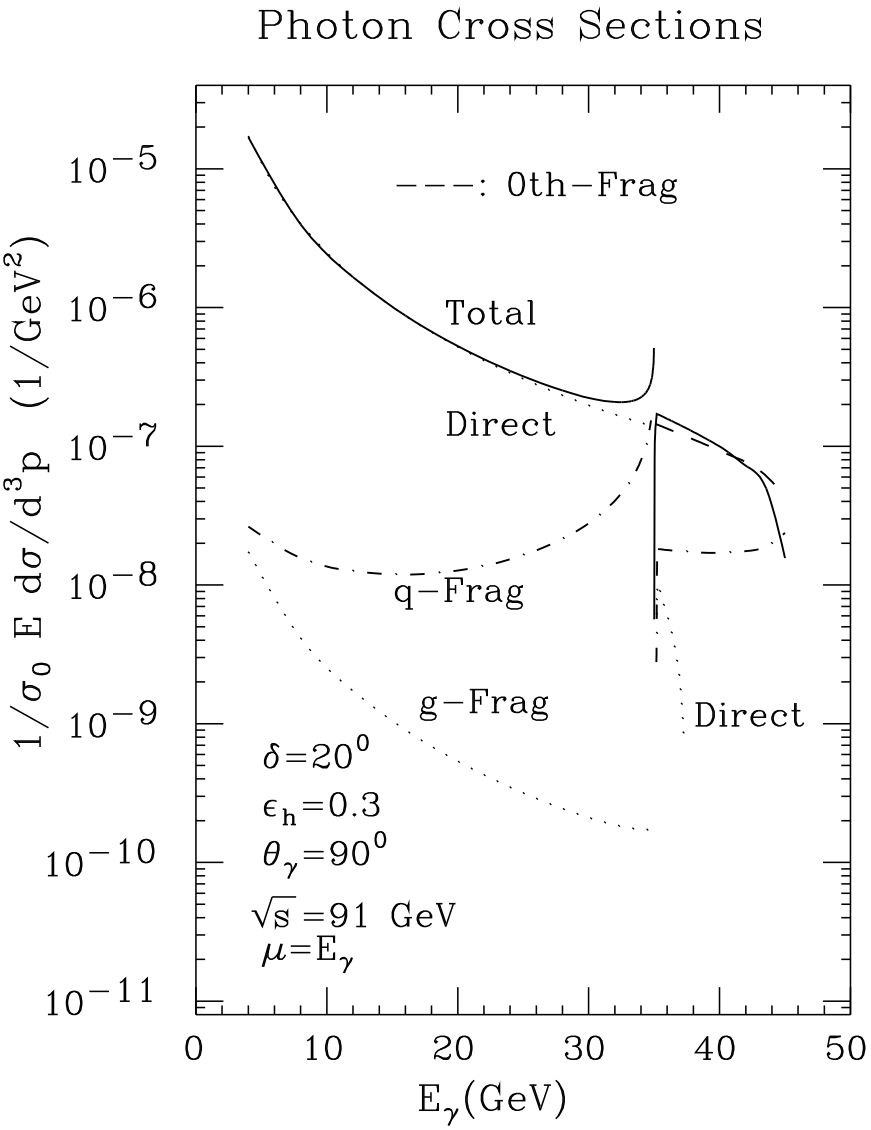
Photon Cross Sections
---: 0th-Frag
Total
Direct
q-Frag
g-Frag
Direct
δ=20^0
ε_h=0.3
θ_γ=90^0
√s =91 GeV
μ=E_γ
1/σ_0 E dσ/d^3p (1/GeV^2)
E_γ(GeV)
10^-5
10^-6
10^-7
10^-8
10^-9
10^-10
10^-11
0
10
20
30
40
50

Fig.12-(b)

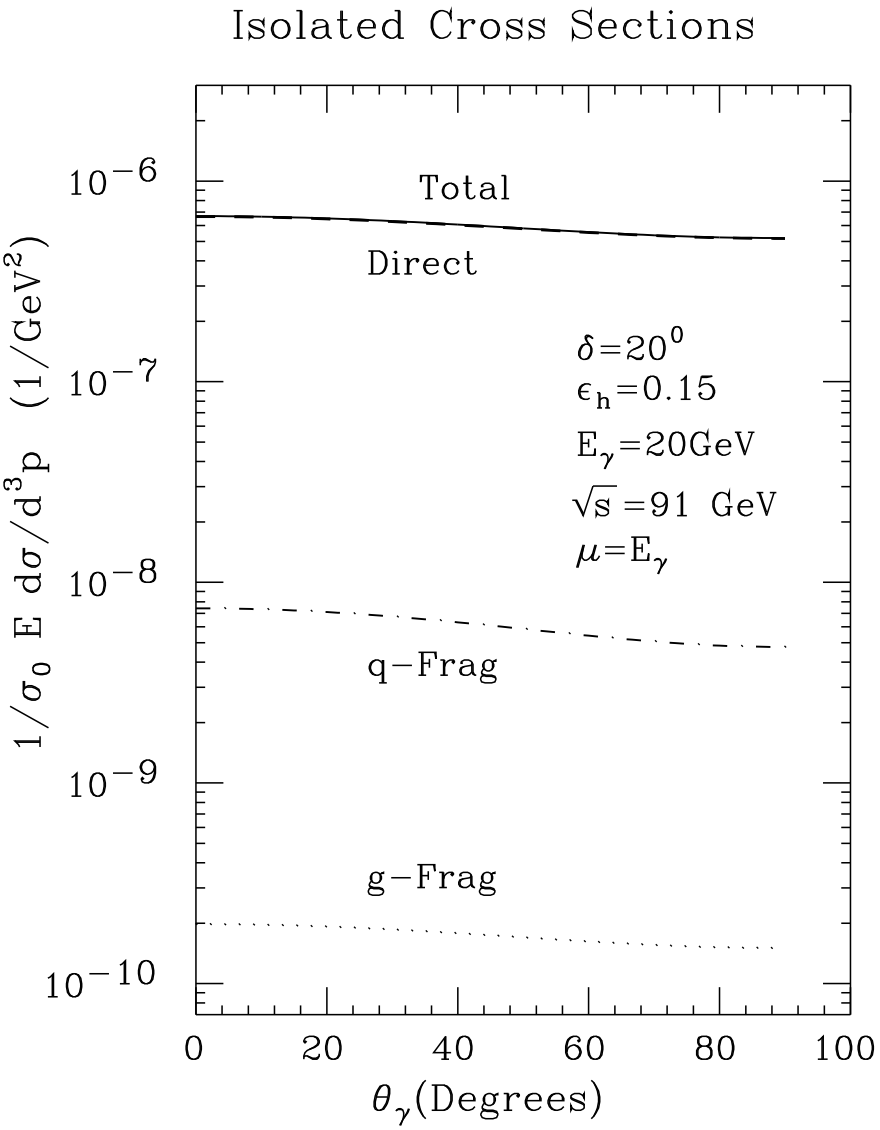
Isolated Cross Sections
Total
Direct
$\delta=20^0$
$\epsilon_h=0.15$
$E_\gamma=20GeV$
$\sqrt{s}=91$ GeV
$\mu=E_\gamma$
q−Frag
g−Frag
$1/\sigma_0\ E\ d\sigma/d^3p\ \ (1/GeV^2)$
10^{-6}
10^{-7}
10^{-8}
10^{-9}
10^{-10}
0
20
40
60
80
100
θ_γ(Degrees)

Fig.13

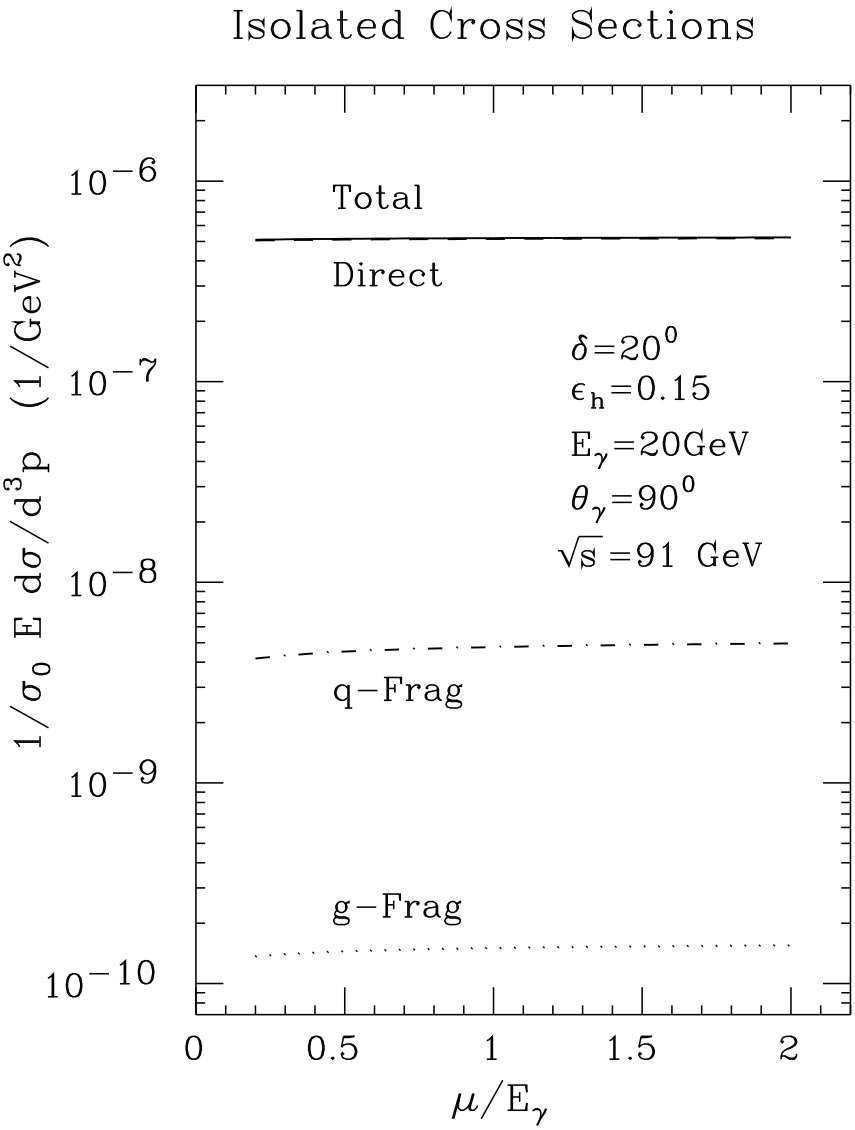
Isolated Cross Sections
Total
Direct
$\delta=20^0$
$\epsilon_h=0.15$
$E_\gamma=20GeV$
$\theta_\gamma=90^0$
$\sqrt{s}=91$ GeV
q−Frag
g−Frag
10^{-6}
10^{-7}
10^{-8}
10^{-9}
10^{-10}
$1/\sigma_0\ E\ d\sigma/d^3p\ \ (1/GeV^2)$
0
0.5
1
1.5
2
μ/E_γ

Fig.14

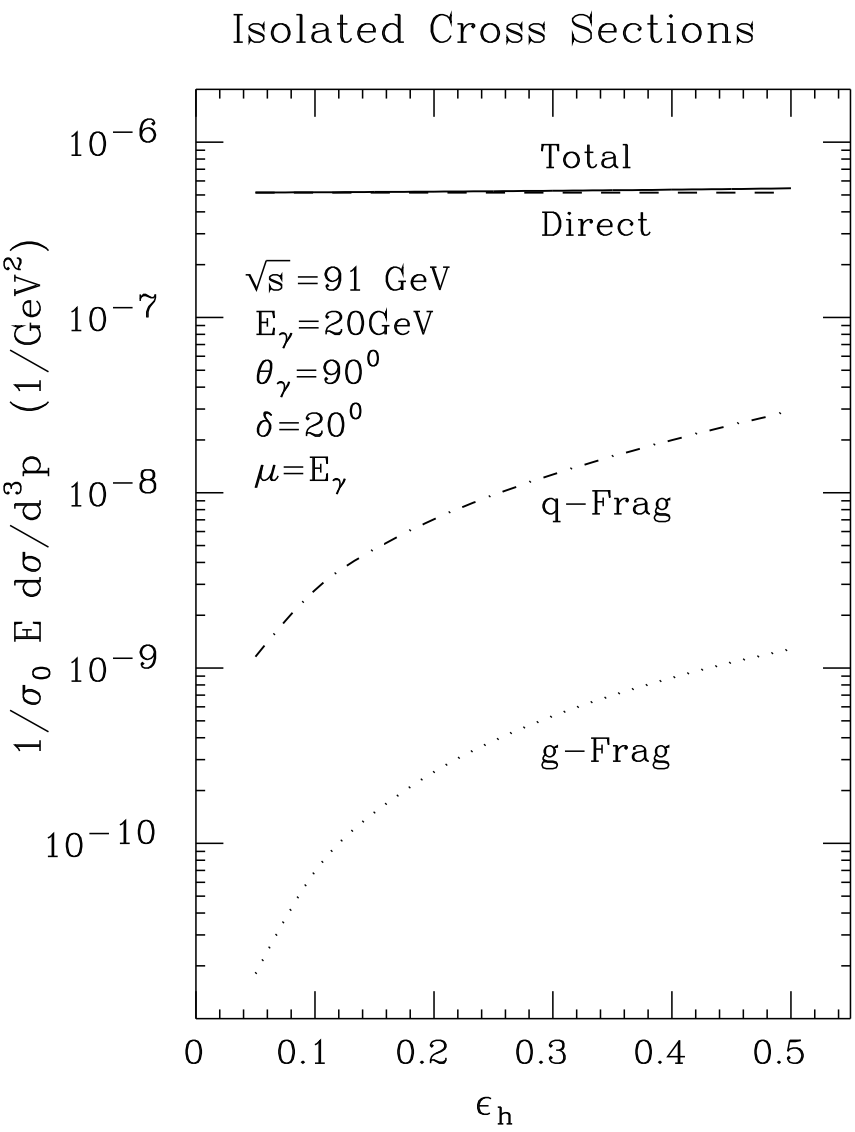
Isolated Cross Sections
Total
Direct
$\sqrt{s}$ =91 GeV
E_γ=20GeV
θ_γ=90^0
δ=20^0
μ=E_γ
q−Frag
g−Frag
10^{-6}
10^{-7}
10^{-8}
10^{-9}
10^{-10}
$1/\sigma_0\ E\ d\sigma/d^3p\ \ (1/GeV^2)$
0
0.1
0.2
0.3
0.4
0.5
ϵ_h

Fig.15

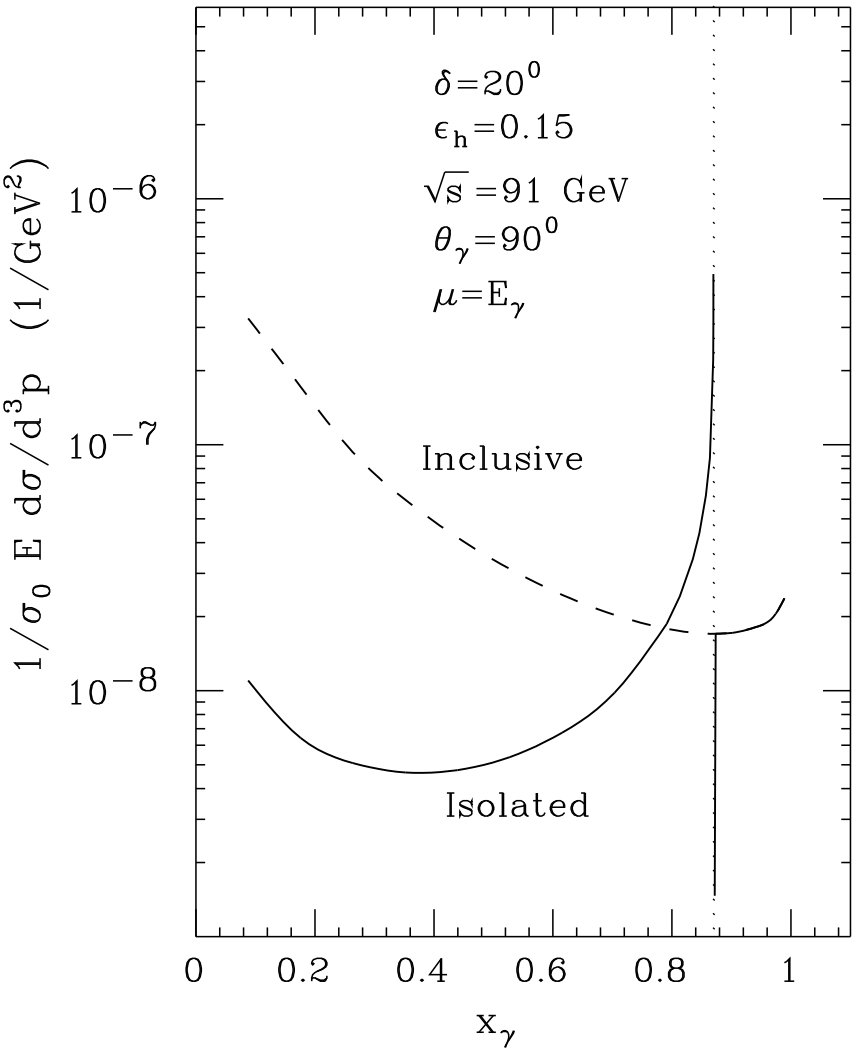
$\delta=20^0$
$\epsilon_h=0.15$
$\sqrt{s}=91$ GeV
$\theta_\gamma=90^0$
$\mu=E_\gamma$
Inclusive
Isolated
$1/\sigma_0\ E\ d\sigma/d^3p\ \ (1/GeV^2)$
10^{-6}
10^{-7}
10^{-8}
0
0.2
0.4
0.6
0.8
1
x_γ

Fig.16

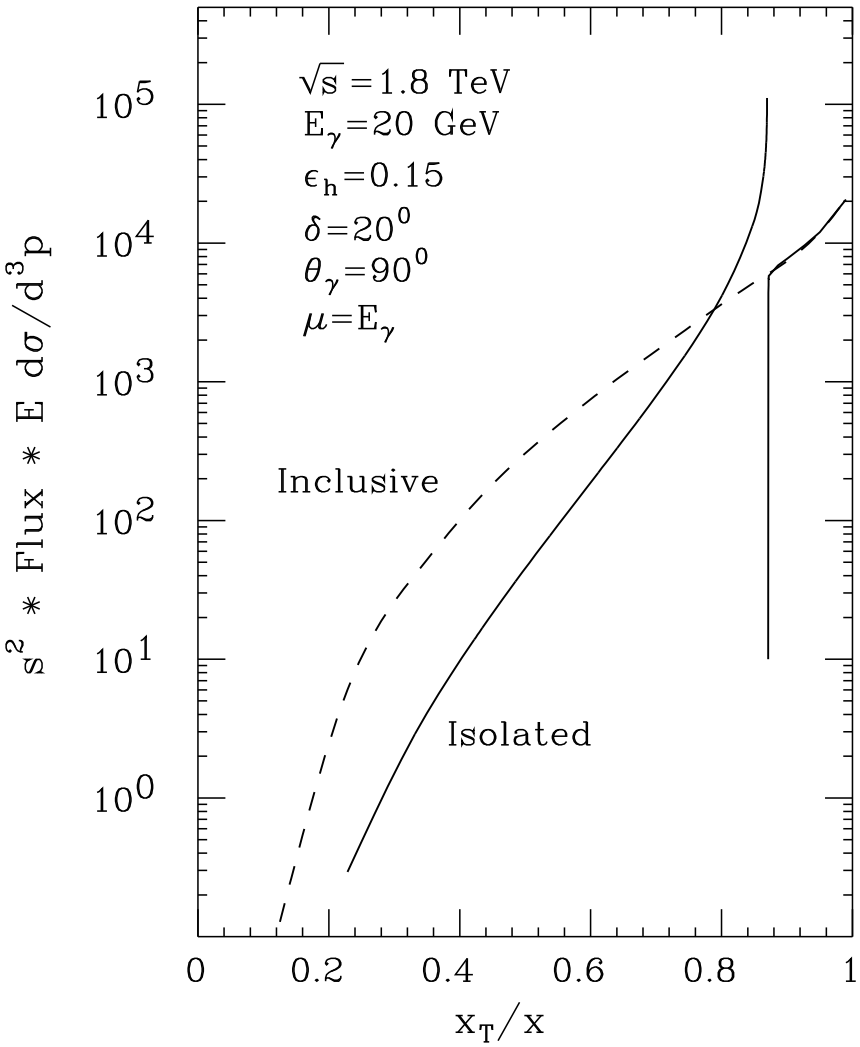
$\sqrt{s}$ =1.8 TeV
E_γ=20 GeV
ϵ_h=0.15
δ=20^0
θ_γ=90^0
μ=E_γ
Inclusive
Isolated
s^2 * Flux * E dσ/d^{3}p
x_T/x
10^0
10^1
10^2
10^3
10^4
10^5
0
0.2
0.4
0.6
0.8
1

Fig.17